

Supporting Information

Dual crosslinked metallopolymers using orthogonal metal complexes as rewritable shape-memory polymers

*Josefine Meurer,^[a, b] Thomas Bätz,^[a, b] Julian Hniopek,^[c, d, e] Stefan Zechel,^[a, b]
Michael Schmitt,^[c, d] Jürgen Popp,^[c, d, e] Martin D. Hager,^[a, b] and Ulrich S. Schubert*^[a, b, d]*

-
- [a] J. Meurer, T. Bätz, Dr. S. Zechel, Dr. M. D. Hager, Prof. U. S. Schubert*
Laboratory of Organic and Macromolecular Chemistry (IOMC)
Friedrich Schiller University Jena
Humboldtstr. 10, 07743 Jena, Germany
E-mail: ulrich.schubert@uni-jena.de
- [b] J. Meurer, T. Bätz, Dr. S. Zechel, Prof. J. Popp, Dr. M. D. Hager, Prof. U. S. Schubert*
Jena Center for Soft Matter (JCSM)
Friedrich Schiller University Jena
Philosophenweg 7, 07743 Jena, Germany
- [c] J. Hniopek, Prof. M. Schmitt, Prof. J. Popp
Institute of Physical Chemistry (IPC)
Friedrich Schiller University Jena
Helmholtzweg 4, 07743 Jena, Germany
- [d] J. Hniopek, Prof. M. Schmitt, Prof. J. Popp, Prof. U. S. Schubert*
Abbe Center of Photonics (ACP)
Friedrich Schiller University Jena
Albert-Einstein-Straße 6, 07745 Jena, Germany
- [e] J. Hniopek, Prof. J. Popp
Leibniz Institute of Photonic Technology (IPHT)
e. V. Jena
Albert-Einstein-Straße 9, 07745 Jena, Germany

Table of Contents

Isothermal titration calorimetry	S3
Synthesis of the model complexes	S5
Synthesis of the polymers P1 and P2 <i>via</i> RAFT polymerization	S6
Size exclusion chromatography	S8
Synthesis of the metallopolymer networks	S9
Differential scanning calorimetry (DSC).....	S10
Thermo gravimetric analysis (TGA).....	S13
Rheology	S15
Frequency sweeps	S15
Thermo mechanical analysis.....	S20
Rewriting investigation.....	S36
Photo series of the shape-memory test	S41
FT-Raman spectroscopy.....	S41
Raman-Spectra of model complexes [(Tpy)₂Fe]²⁺ and [(His)₃Fe]²⁺	S42
Composition analysis by picture analysis	S48
References	S49

Isothermal titration calorimetry

All titrations were performed using a standard volume Nano ITC (TA Instruments) at 303 K. Solutions were always prepared prior to use in dry solvents using vacuum dried ligand and metal salt. Blank titrations in dry solvent were performed and subtracted from the corresponding titrations to remove the effect of dilution. The fitting of the measured data was performed with the NanoAnalyze program from TA instruments. For the titration experiments with the histidine ligand a previously synthesized model compound (**His**) was used, which was synthesized according to literature.^{1,2}

The ITC measurements of Zn(TFMS)₂ and NiCl₂ were already presented in a former study³ and are presented here again for the sake of completeness. The measurement of terpyridine and NiCl₂ was additionally repeated to obtain a better resolution. Therefore, more measurement points in the titration region were utilized enabling a more exact value of the complexation formation constant. The titration of FeSO₄ with the histidine ligand revealed an extremely low association constant. Thus, a detailed analysis of the results was not performed since those values would not be trustable.

Table S1. Determined complex association constants (K_a) and stoichiometry (n) for **Tpy** or **His** and different metal salts by ITC measurements.

Metal salt(s)	Ligand	K_a	n	Reference
Zn(TFMS) ₂		6.02×10^2	2.23	[3]
NiCl ₂	His	2.84×10^2	3.71	[3]
FeSO ₄		-	-	-
Zn(TFMS) ₂		3.24×10^6	1.90	[3]
NiCl ₂	Tpy	2.43×10^7	2.24	[3]
FeSO ₄		1.00×10^{10}	1.91	-

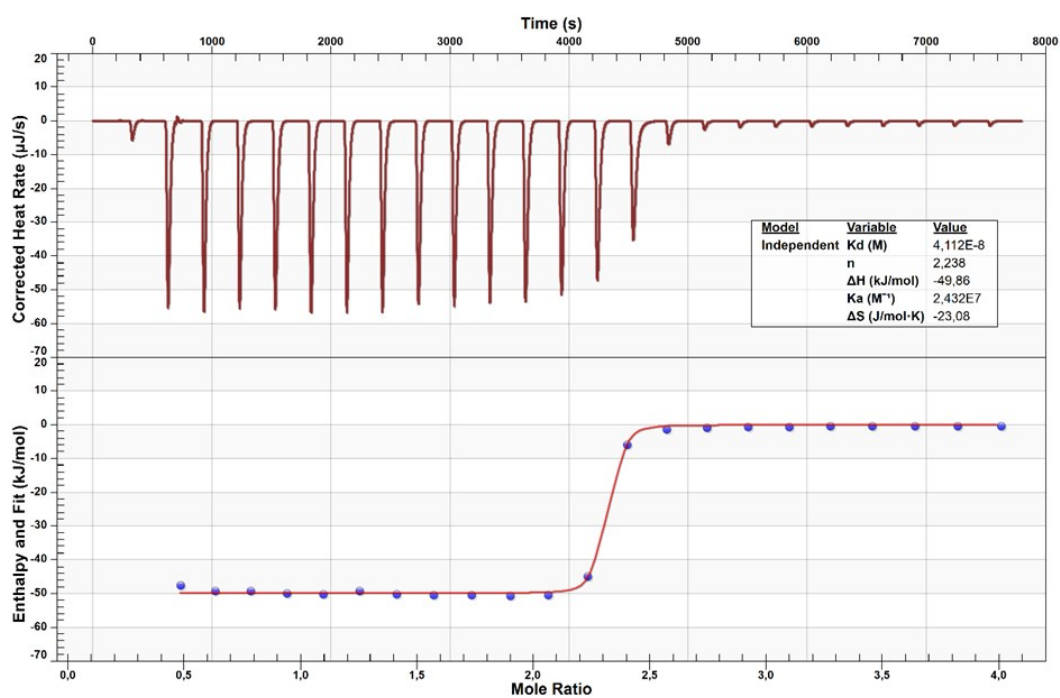


Figure S1. ITC titration data of $\text{NiCl}_2 \times 6 \text{H}_2\text{O}$ (0.25 mM, in cell) with **Tpy** (3.43 mM, in syringe) in $\text{MeOH}/\text{CHCl}_3$ (2:1) at 303 K.

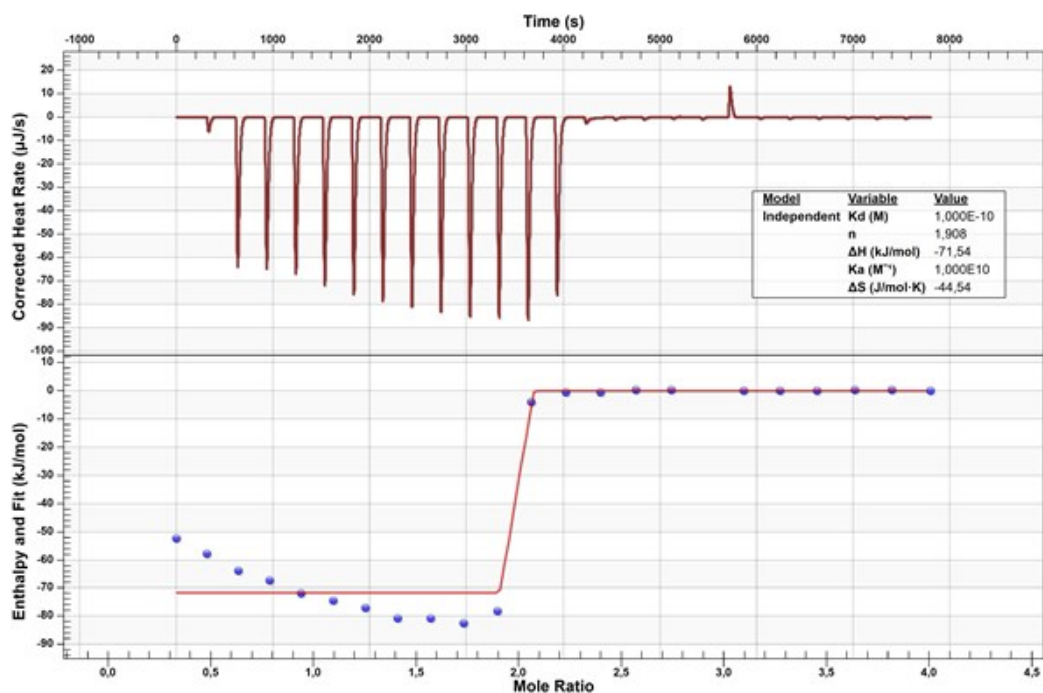


Figure S2. ITC titration data of $\text{FeSO}_4 \times 7 \text{H}_2\text{O}$ (0.214 mM, in cell) with **Tpy** (3.42 mM, in syringe) in $\text{MeOH}/\text{CHCl}_3$ (2:1) at 303 K.

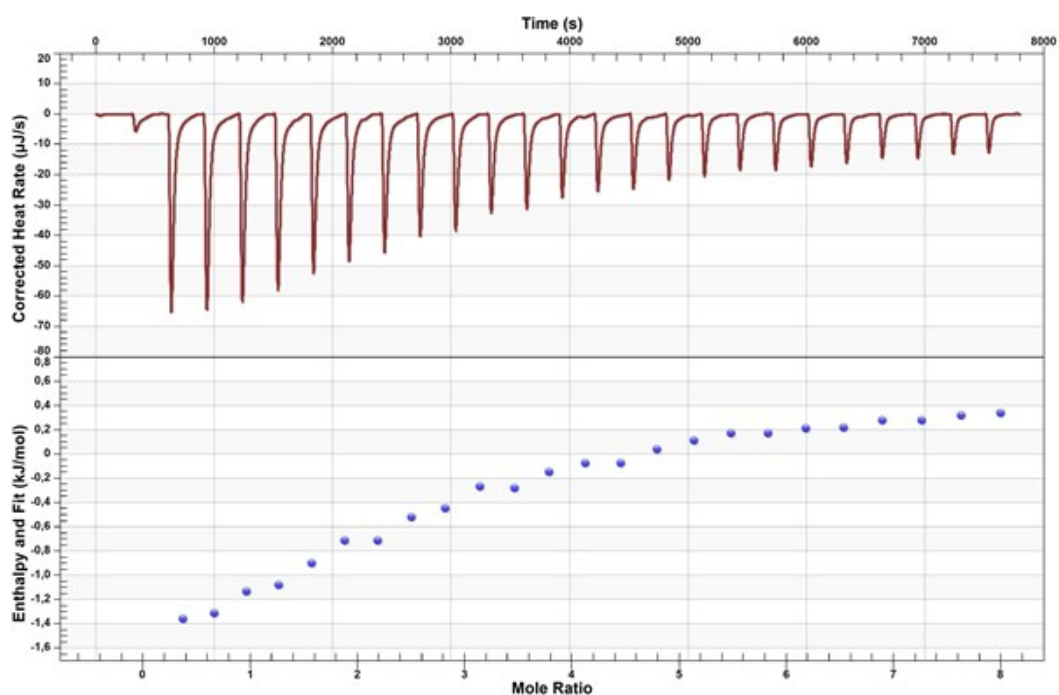


Figure S3. ITC titration data of $\text{FeSO}_4 \times 7 \text{H}_2\text{O}$ (6.25 mM, in cell) with **His** (170.9 mM, in syringe) in $\text{MeOH}/\text{CHCl}_3$ (2:1) at 303 K.

Synthesis of the model complexes

The synthesis of the model compounds $[(\text{His})_2\text{Zn}]^{2+}$, $[(\text{Tpy})_2\text{Zn}]^{2+}$, $[(\text{His})_3\text{Ni}]^{2+}$ and $[(\text{Tpy})_2\text{Ni}]^{2+}$ was already presented in an earlier study.³ The synthesis of the model compounds $[(\text{His})_2\text{Fe}]^{2+}$ and $[(\text{Tpy})_2\text{Fe}]^{2+}$ was performed analogously. The ligand was dissolved in chloroform (10 mL). The $\text{FeSO}_4 \times 7 \text{H}_2\text{O}$ was dissolved in methanol (2 mL) and added to the dissolved ligand. The solution was stirred for 10 minutes. Afterward the solvent was evaporated. The resulting model complex was dried *in vacuo* at 40 °C overnight. The utilized quantities of the metal salt ($\text{FeSO}_4 \times 7 \text{H}_2\text{O}$) and the respective ligand are summarized in **Table S2**.

Table S2. Utilized masses and volumes for the synthesis of the model complexes $[(\text{His})_2\text{Fe}]^{2+}$ and $[(\text{Tpy})_2\text{Fe}]^{2+}$.

Metallopolymer	Ligand	m [mg] (ligand)	Metal salt	m [mg] (metal salt)
$[(\text{His})_2\text{Fe}]^{2+}$	His	100	$\text{FeSO}_4 \times 7 \text{H}_2\text{O}$	18
$[(\text{Tpy})_2\text{Fe}]^{2+}$	Tpy	200		119

Synthesis of the polymers **P1** and **P2** via RAFT polymerization

All polymerizations were performed in a 100 mL one-neck-round bottom flask. 2,2'-Azobis(2-methylpropionitrile) (AIBN) as initiator, 2-cyano-2-propyl dodecyl trithiocarbonate (CPDT) as chain transfer agent as well as the monomers *N*^α-methacryloyl-*N*^ε-tritylhistidine butyl amide (**His-MA**), 6-(2,2':6'2''-terpyridin-4'-yloxy)-hexyl methacrylate (**Tpy-MA**) and the main monomer (2-ethyl hexyl methacrylate (2-EHMA) or butyl methacrylate (BMA)), respectively, were added into the flask. Subsequently, the required amount of toluene was added to reach the desired concentration of 2 M. The [Monomer] to [CPDT] ratio was 125/1, the ratio of [CPDT] to [AIBN] 4/1. The respective utilized quantities of all substances are listed in **Table S3**. The solution was purged with nitrogen for 1 h. Afterwards, the mixture was stirred for 17 h in a preheated oil bath at 70 °C. The crude product was purified by the use of dialysis (MWCO: 3500 g/mol, THF). The solvent was changed two times each day for three days. Additionally, a model polymer (**P_M**) was synthesized according to the synthesis of the polymers **P1** and **P2** bearing only the terpyridine ligand. The ¹H NMR spectra of the polymers **P1** and **P2** are shown in **Figure S9**. The results of the elemental analysis and the differential scanning calorimetry and thermo gravimetric analysis are summarized in **Table S4**.

Table S3. Utilized masses and volumes for the copolymerization of the polymers **P1** and **P2**.

Polymer	Monomer	m [g] (monomer)	m [mg] (AIBN)	m [mg] (CPDT)	V [mL] (toluene)
P1	2-EHMA	14.00			
	His-MA	3.68	27.0	224.0	40.6
	Tpy-MA	3.53			
P2	BMA	14.00			
	His-MA	5.13	37.0	313.0	56.6
	Tpy-MA	4.92			
P_M	BMA	4			
	His-MA	-	9.7	81.7	14.8
	Tpy-MA	0.587			

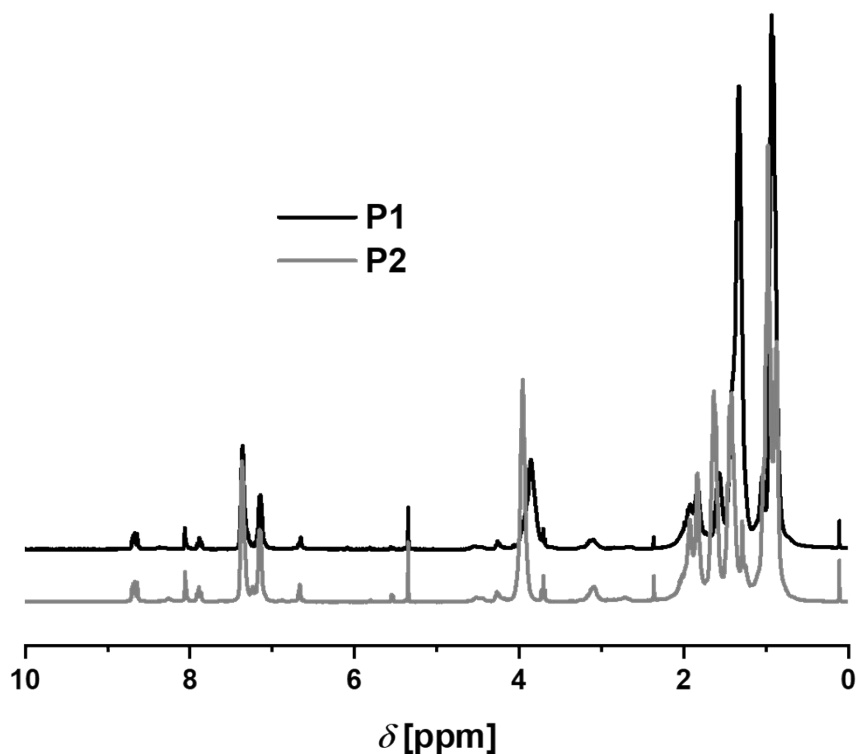


Figure S4. ¹H NMR spectra of the polymers **P1** (black) and **P2** (grey) (300 MHz, CD₂Cl₂).

Table S4. Calculated composition *via* ¹H NMR, determined molar masses and dispersity *via* SEC, determined thermal properties *via* DSC and TGA investigations and results of the elemental analysis.

	Calculated composition <i>via</i> ¹ H NMR [a]		SEC results [b]			Thermal properties		Elemental analysis [%]			
	His [%]	Tpy [%]	M _n [g mol ⁻¹]	M _w [g mol ⁻¹]	Đ	T _g [°C]	T _d [°C]	C	H	N	S
P1 (2-EHMA)	7	3.5	17 100	20 200	1.28	- 8.9	261	Calc: 69.49 Found: 72.48	9.12 9.98	2.76 2.51	-
P2 (BMA)	6	4.0	13 900	17 800	1.28	37.5	223	Calc: 69.37 Found: 68.87	9.14 8.85	2.66 3.14	-
P_M (BMA)	-	4.1	11 500	14 900	1.29	-	213	Calc: - Found: -	- -	- -	-

[a] CD₂Cl₂. 300 MHz. [b] Solvent: CHCl₃/*i*-PrOH/NEt₃ (94/2/4), PMMA-standard.

Size exclusion chromatography

Size exclusion chromatography measurements were performed on the following setup: Shimadzu with CBM-20A (system controller), DGU-14A (degasser), LC-20AD (pump), SIL-20AHT (auto sampler), CTO-10AC vp (oven), SPD-20A (UV detector), RID-10A (RI detector), PSS SDV guard/1000 Å/1,000,000 Å (5 µm particle size) chloroform/isopropanol/triethylamine [94/2/4] with 1 mL/min at 40 °C, poly(methyl methacrylate) (standard).

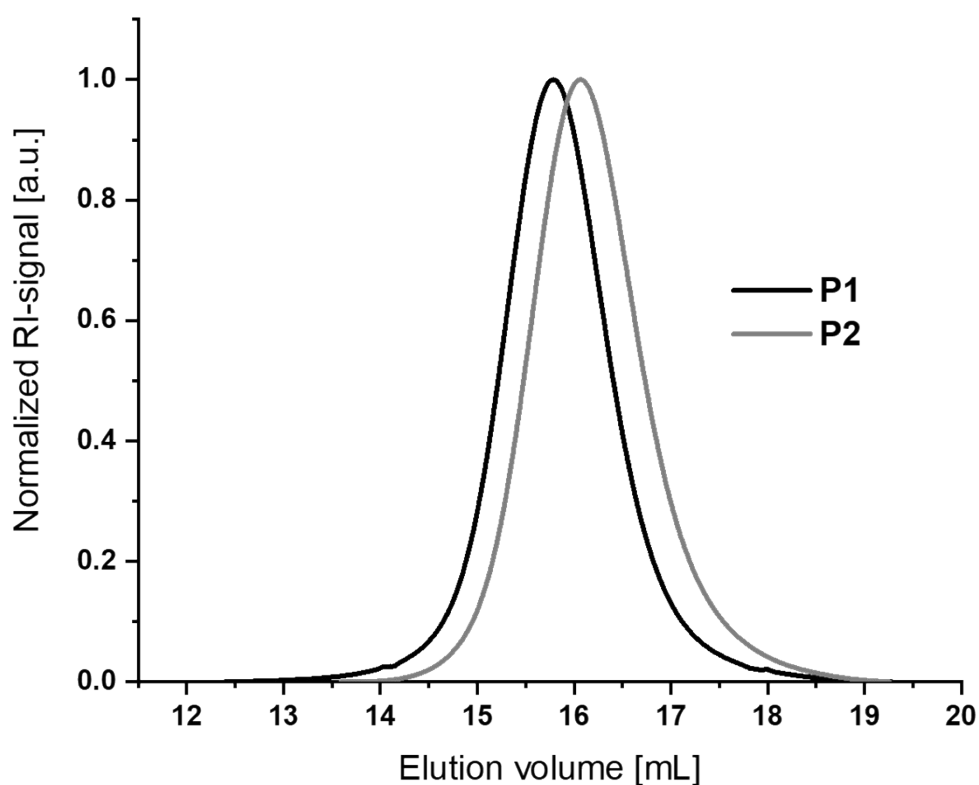


Figure S5. SEC curves of the polymers **P1** (black) and **P2** (grey) (eluent: Chloroform/isopropanol/triethylamine [94/2/4]).

Synthesis of the metallopolymer networks

For the synthesis of the metallopolymer networks (**P1-Fe/Zn** and **P2-Fe/Zn**; **P1-Ni/Zn** and **P2-Ni/Zn**; **P1-Fe/Ni** and **P2-Fe/Ni**), the polymer (**P1** or **P2**) was dissolved in chloroform (50 mL). The respective amount of the metal salts were (separately) weight in and individually dissolved in methanol (2 mL). Afterwards, under stirring the polymer solution, the dissolved salt for the formation of the stable terpyridine complex was added, followed by the addition of the salt-solution for the formation of the labile histidine complex. Subsequently, according to the synthesis of the metallopolymer networks, FeSO₄ and NiCl₂, respectively, was added to the polymer to obtain the model metallopolymer networks **P_M-Fe** and **P_M-Ni**.

The solvent was evaporated and the resulting metallopolymer networks were dried *in vacuo* at 40 °C. The respective used quantities of all substances are listed in **Table S5**. The results of the elemental analysis and the TGA measurements are summarized in **Table S6**. In order to perform shape-memory tests and rheology measurements with the metallopolymer networks, they were pressed in a manufactured mold at a temperature of about 150 °C at a weight force of about 2 t in a rectangular shape.

Table S5. Utilized masses and volumes for the synthesis of the metallopolymer networks.

Metallopolymer	Polymer	m [g] (polymer)	Metal salt (Tpy-complex)	m [mg] (metal salt for Tpy-complex)	Metal salt (His-complex)	m [mg] (metal salt for His-complex)
P1-Fe/Zn		1.56	FeSO ₄ × 7 H ₂ O	77	Zn(TFMS) ₂	203
P1-Ni/Zn	P1	1.53	NiCl ₂ × 6 H ₂ O	66	Zn(TFMS) ₂	203
P1-Fe/Ni		2.25	FeSO ₄ × 7 H ₂ O	77	NiCl ₂ × 6 H ₂ O	88
P2-Fe/Zn		1.55	FeSO ₄ × 7 H ₂ O	115	Zn(TFMS) ₂	233
P2-Ni/Zn	P2	1.53	NiCl ₂ × 6 H ₂ O	98	Zn(TFMS) ₂	233
P2-Fe/Ni		1.51	FeSO ₄ × 7 H ₂ O	115	NiCl ₂ × 6 H ₂ O	101
P_M-Fe	P_M	1.2	NiCl ₂ × 6 H ₂ O	0.037	-	-
P_M-Fe	P_M-Fe	1.2	FeSO ₄ × 7 H ₂ O	0.044	-	-

Table S6. Results of the elemental analysis and the TGA investigations of the metallopolymer networks **P1-Fe/Zn**, **P2-Fe/Zn**, **P1-Ni/Zn**, **P2-Ni/Zn**, **P1-Fe/Ni** and **P2-Fe/Ni**.

Polymer		Elemental analysis [%]				T_d [°C]
		C	H	N	S	
P1-Fe/Zn	Calc.:	65.15	8.50	2.57	1.36	253
	Found:	68.45	9.34	2.44	1.19	
P2-Fe/Zn	Calc.:	65.26	8.55	2.48	1.29	262
	Found:	64.51	8.24	3.01	1.54	
P1-Ni/Zn	Calc.:	65.28	8.51	2.58	1.09	257
	Found:	69.46	9.49	2.49	0.94	
P2-Ni/Zn	Calc.:	65.41	8.57	2.49	0.97	244
	Found:	65.13	8.34	3.02	1.13	
P1-Fe/Ni	Calc.:	67.53	8.86	2.68	0.28	230
	Found:	70.48	9.73	2.53	0.43	
P2-Fe/Ni	Calc.:	66.93	8.82	2.56	0.33	257
	Found:	66.48	8.58	3.11	0.60	

Differential scanning calorimetry (DSC)

Differential scanning calorimetry (DSC) was measured utilizing a Netzsch DSC 204 F1 Phoenix instrument (Selb, Germany) under a nitrogen atmosphere with a heating rate of 20 K min⁻¹ (first and second heating cycle) and 10 K min⁻¹ (third heating cycle). In general, the first cycle is used as annealing step and to delete the thermal history of the sample and is, therefore, neglected.

The DSC investigations revealed that the determined glass transition temperatures (T_g) of the metallopolymer networks are significant higher compared to those of the respective linear polymer. Furthermore, in some case, small endothermic signals occur at temperatures about 70 to 90 °C and in a range from 110 to 130 °C. Those peaks may result from the activation of the two different metal complexes, which could not finally be proven up to now.

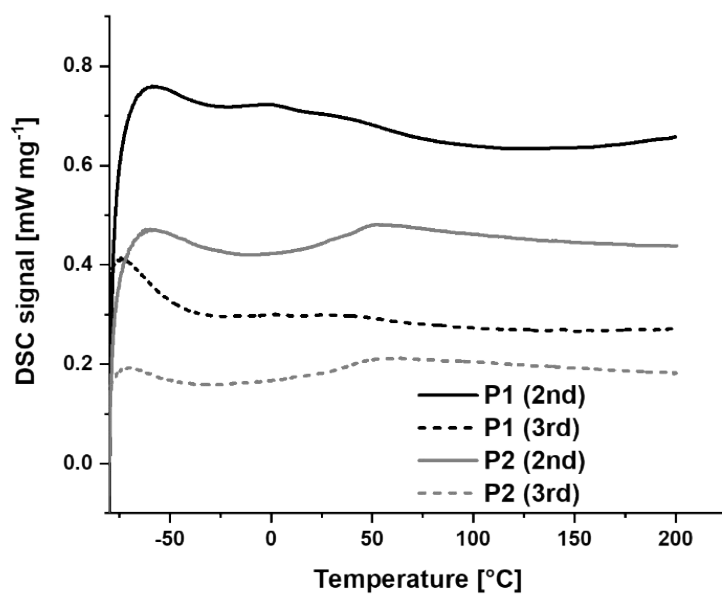


Figure S6. DSC-curves of the second (straight) and third (dotted) heating cycle of the polymers **P1** (black) and **P2** (grey).

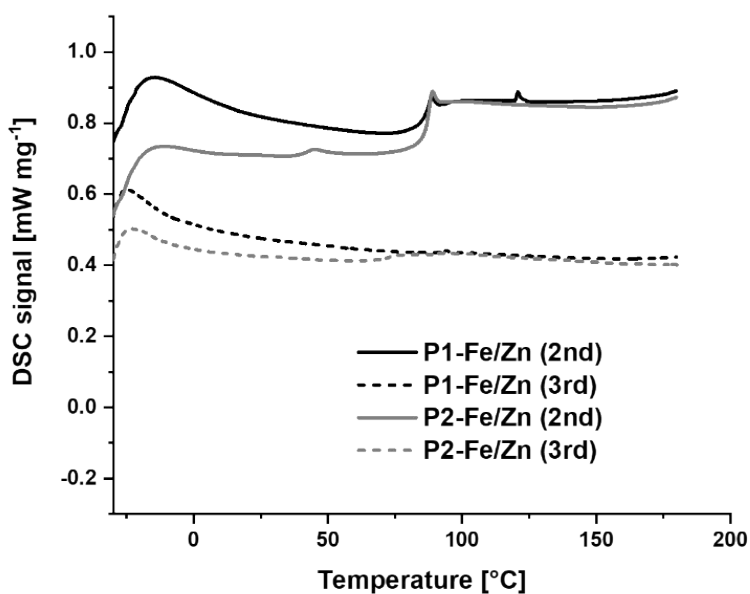


Figure S7. DSC-curves of the second (straight) and third (dotted) heating cycle of the metallopolymer networks **P1-Fe/Zn** (black) and **P2-Fe/Zn** (grey).

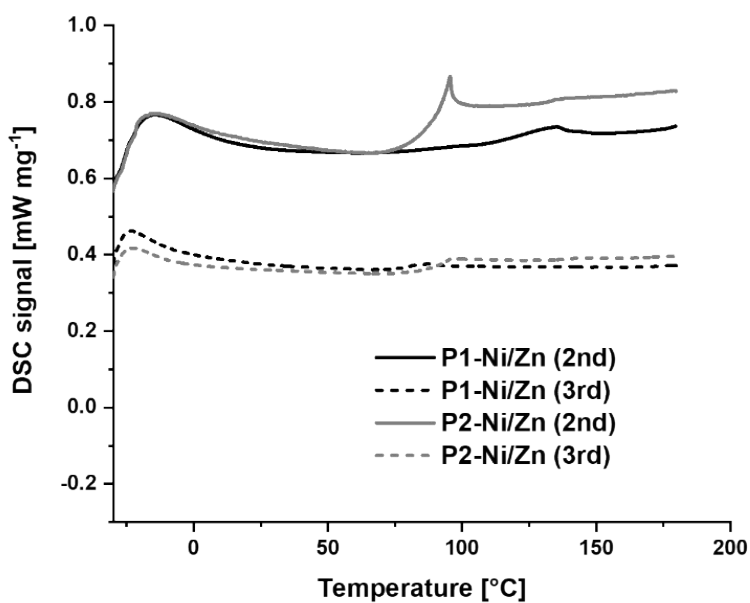


Figure S8. DSC-curves of the second (straight) and third (dotted) heating cycle of the metallopolymer networks **P1-Ni/Zn** (black) and **P2-Ni/Zn** (grey).

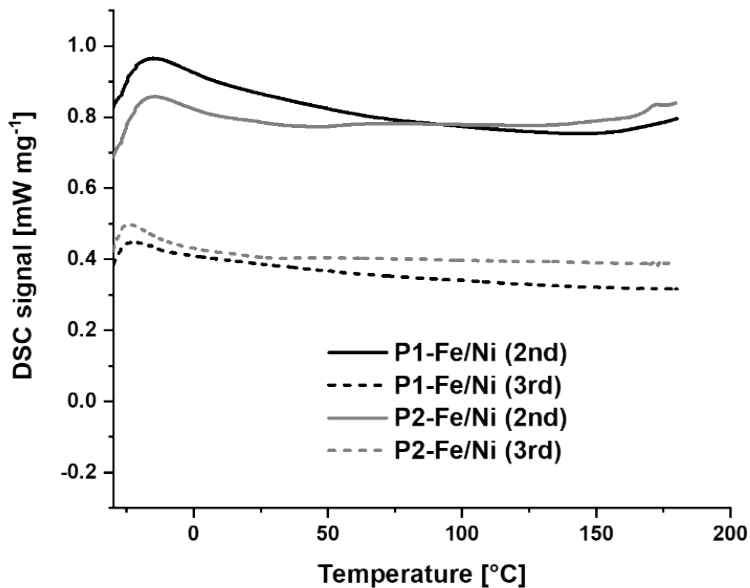


Figure S9. DSC-curves of the second (straight) and third (dotted) heating cycle of the metallopolymer networks **P1-Fe/Ni** (black) and **P2-Fe/Ni** (grey).

Thermo gravimetric analysis (TGA)

The thermogravimetric analysis (TGA) was carried under normal atmosphere using a Netzsch TG 209 F1 Iris (Selb, Germany) with a heating rate of 10 K min^{-1} from 25 to $600 \text{ }^\circ\text{C}$. The thermo gravimetric analysis revealed degradation temperatures above $220 \text{ }^\circ\text{C}$ for all synthesized polymers and metallopolymer networks.

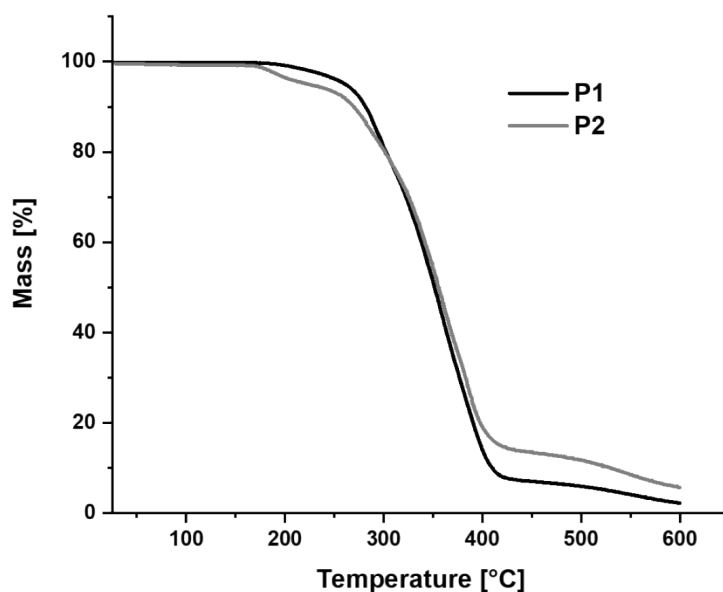


Figure S10. TGA-curves of the polymers **P1** (black) and **P2** (grey).

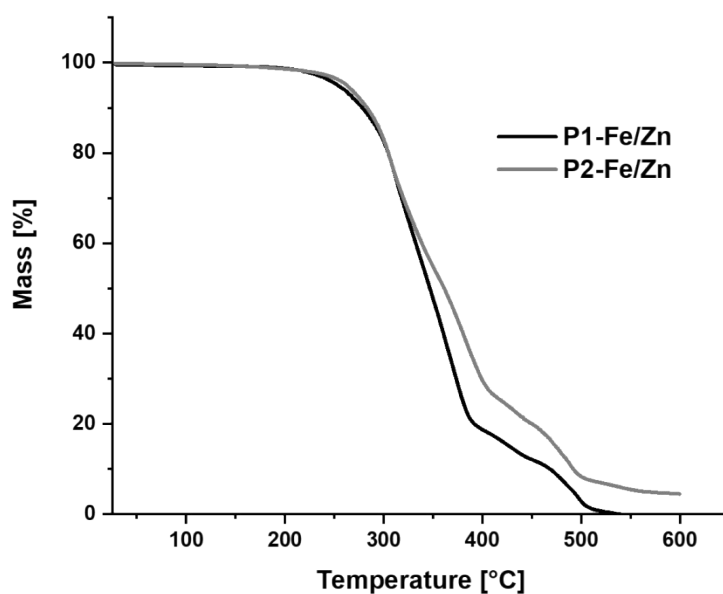


Figure S11. TGA-curves of the metallopolymer networks **P1-Fe/Zn** (black) and **P2-Fe/Zn** (grey).

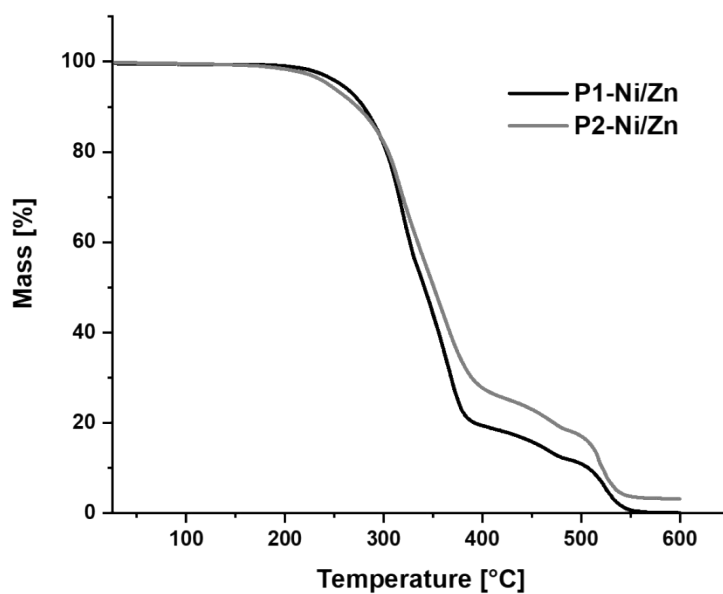


Figure S12. TGA-curves of the metallopolymer networks **P1-Ni/Zn** (black) and **P2-Ni/Zn** (grey).

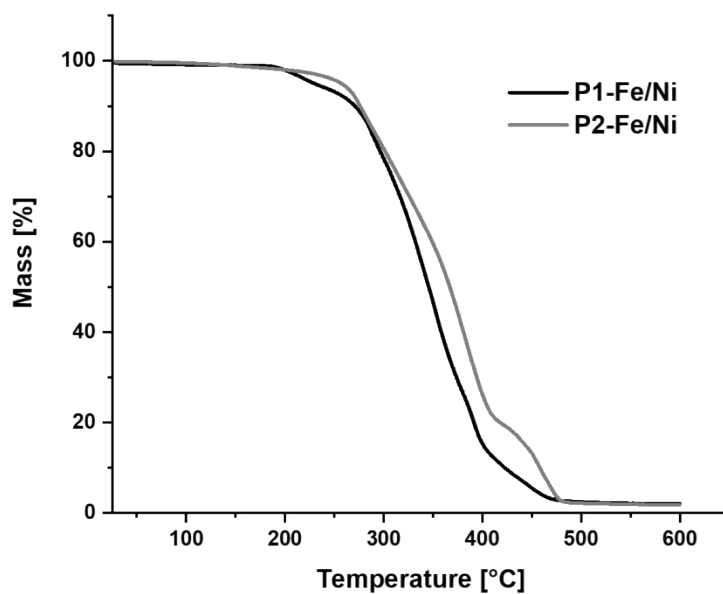


Figure S13. TGA-curves of the metallopolymer networks **P1-Fe/Ni** (black) and **P2-Fe/Ni** (grey).

Rheology

All rheology measurements were performed utilizing a MCR 301 rheometer from Anton Paar (Graz, Austria) using the convection oven device CTD 450. The samples were measured with a solid rectangular fixture setup (SRF12-SN13529, Anton Paar (Graz, Austria) in dimensions of approximately 29 × 10 mm (length, width) and a thickness of approx. 1.5–3.5 mm. The resulting sample gap was set to 15 to 20 mm.

The software RheoCompass™ V1.24.549-Release 64-bit (Anton Paar, Graz, Austria) was applied for the operating of the rheometer as well as for analysis. The data was exported as txt-files and evaluated and processed with OriginPro 2019 (OriginLab Corporation, Northampton, MA, USA).

Frequency sweeps

The temperature was set to the desired value. The frequency was decreased in a logarithmic profile from 100 down to 0.001 Hz at a constant oscillating shear strain (0.1%, 0.05% or 0.01% respectively) and a constant temperature. The resulting plots are shown in **Figure S19 to S24**. The crossovers of G' and G'' as well as the corresponding bond lifetimes are summarized in **Table S7**.

$$\text{Supramolecular bond lifetime} = 1/\text{frequency (crossover)} \quad (\text{S1})$$

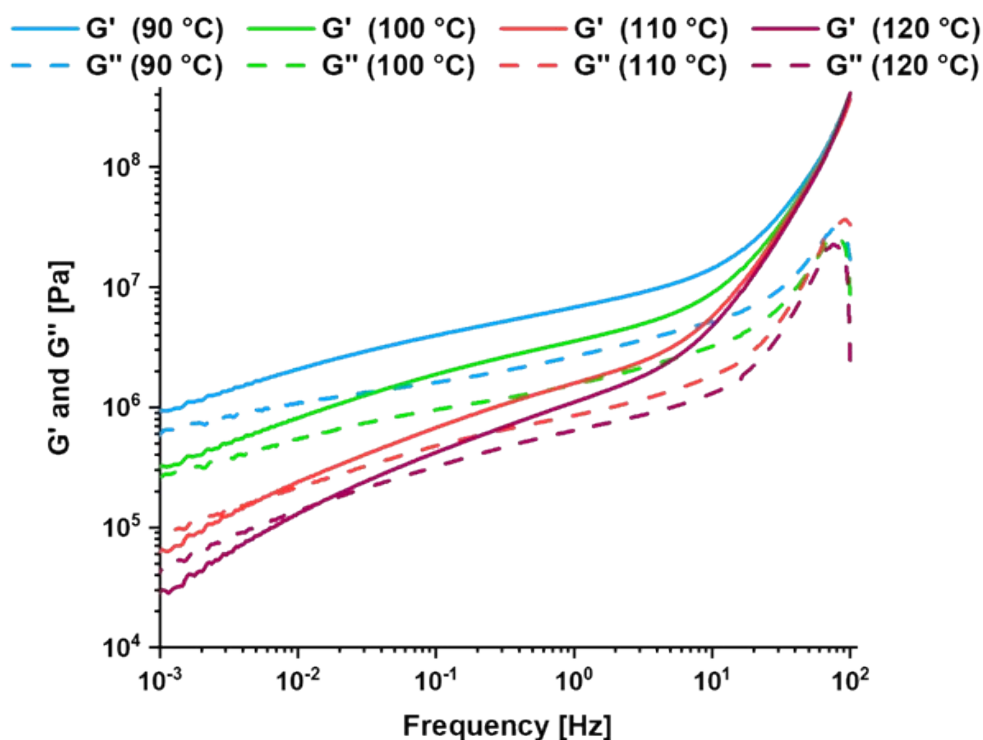


Figure S14. Frequency sweep DMA of the metallopolymer network P1-Fe/Zn at different temperatures (90 °C (blue); 100 °C (green); 110 °C (orange); 120 °C (dark red)).

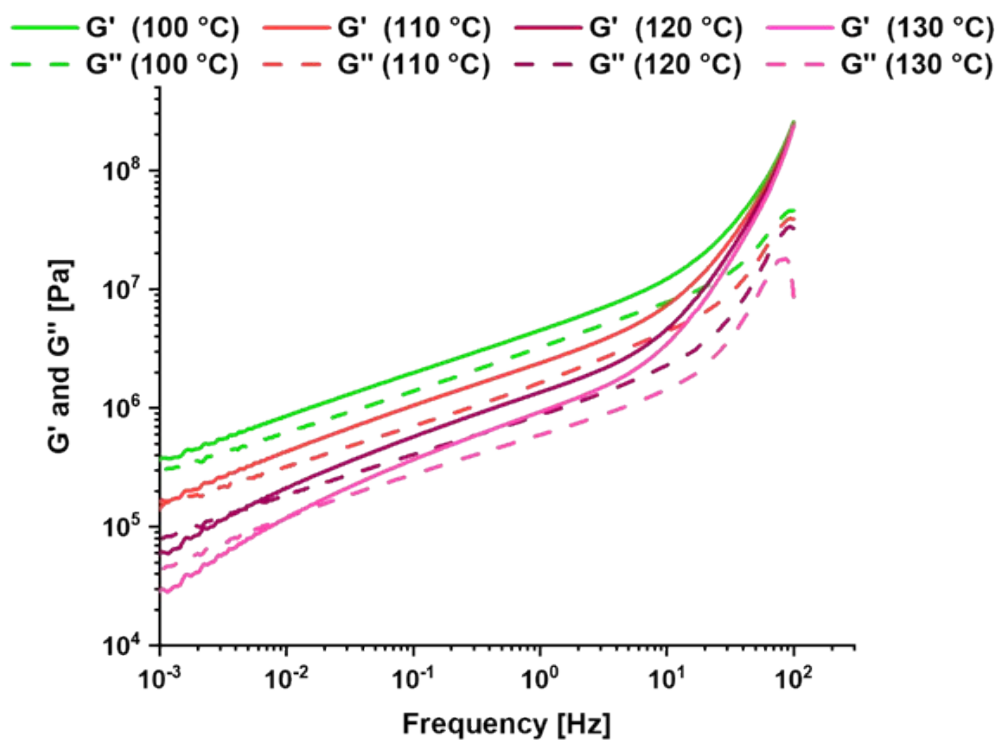


Figure S15. Frequency sweep DMA of the metallopolymer network **P2-Fe/Zn** at different temperatures (100 °C (green); 110 °C (orange); 120 °C (dark red); 130 °C (pink)).

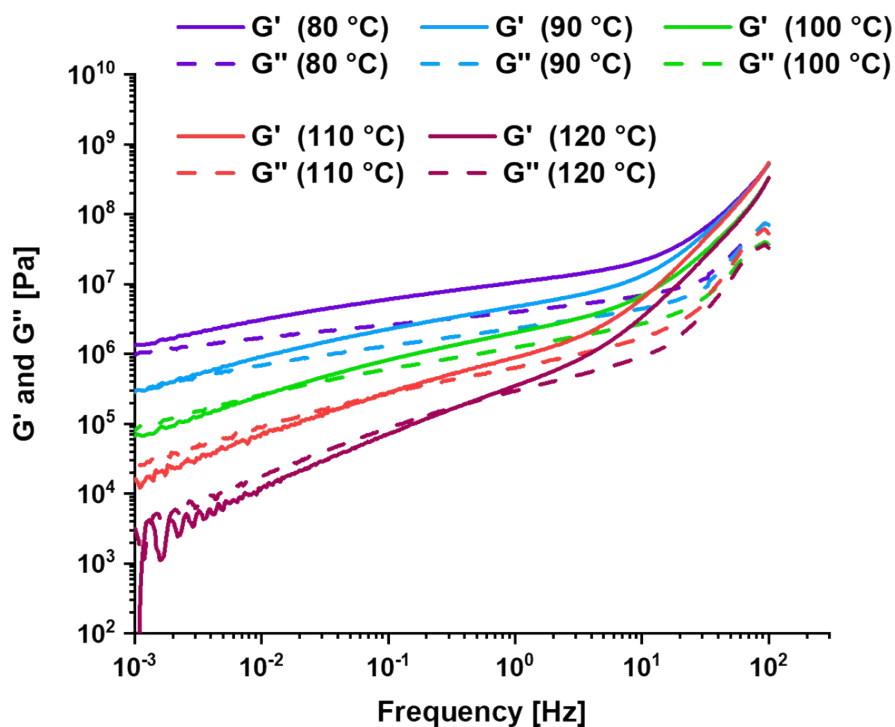


Figure S16. Frequency sweep DMA of the metallopolymer network **P1-Ni/Zn** at different temperatures (80 °C (purple); 90 °C (blue); 100 °C (green); 110 °C (orange); 120 °C (dark red)).

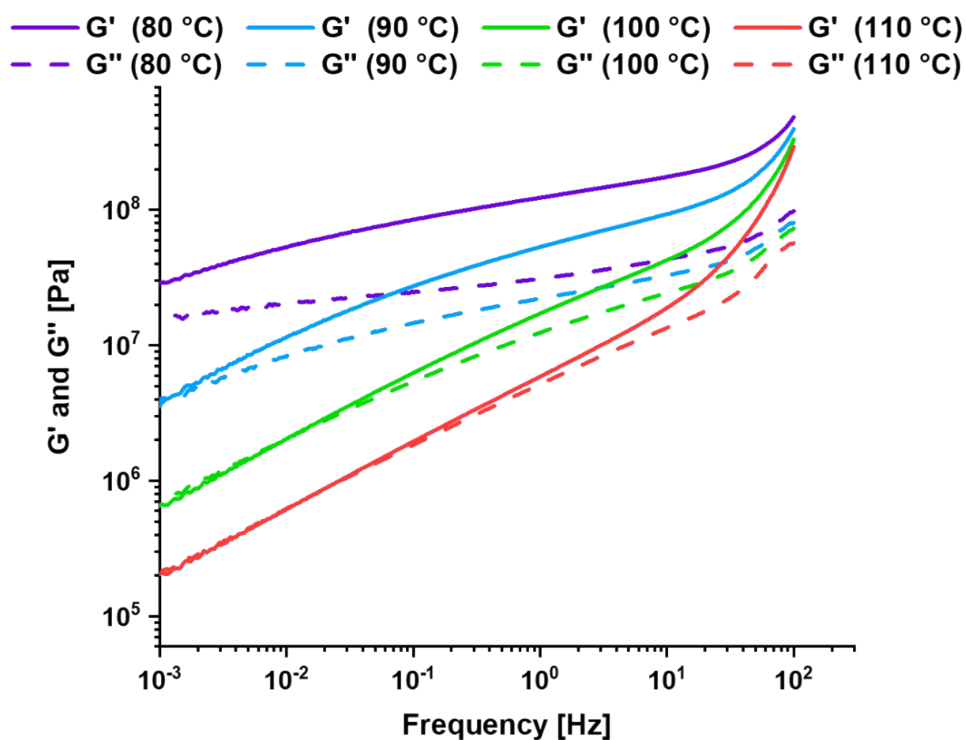


Figure S17. Frequency sweep DMA of the metallopolymer network **P2-Ni/Zn** at different temperatures (80 °C (purple); 90 °C (blue); 100 °C (green); 110 °C (orange)).

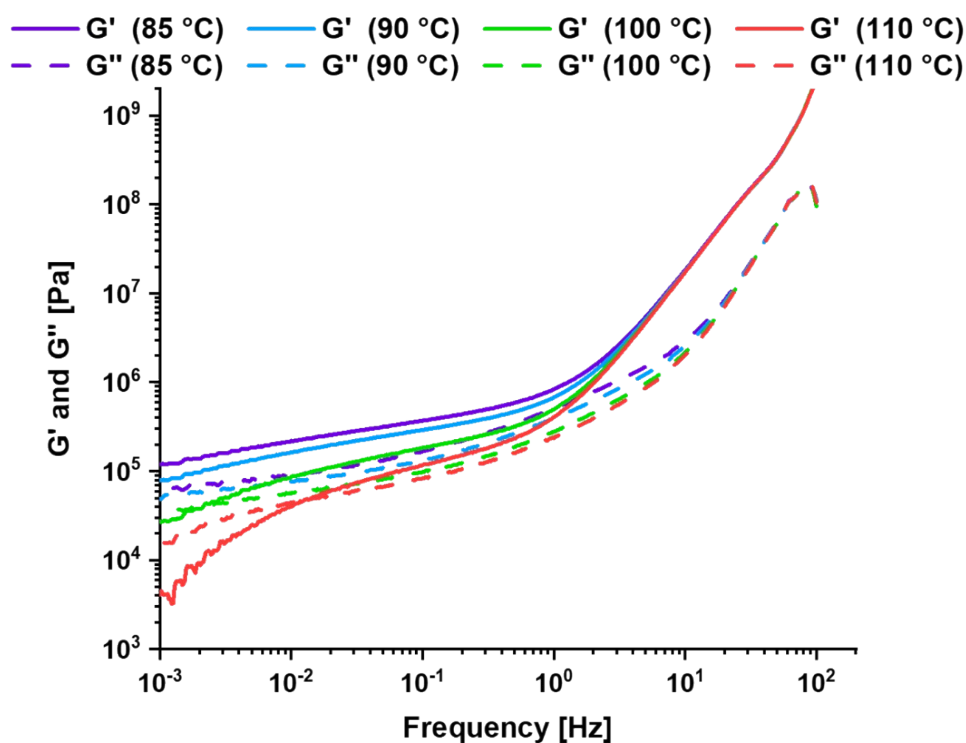


Figure S18. Frequency sweep DMA of the metallopolymer network **P1-Fe/Ni** at different temperatures (85 °C (purple); 90 °C (blue); 100 °C (green); 110 °C (orange)).

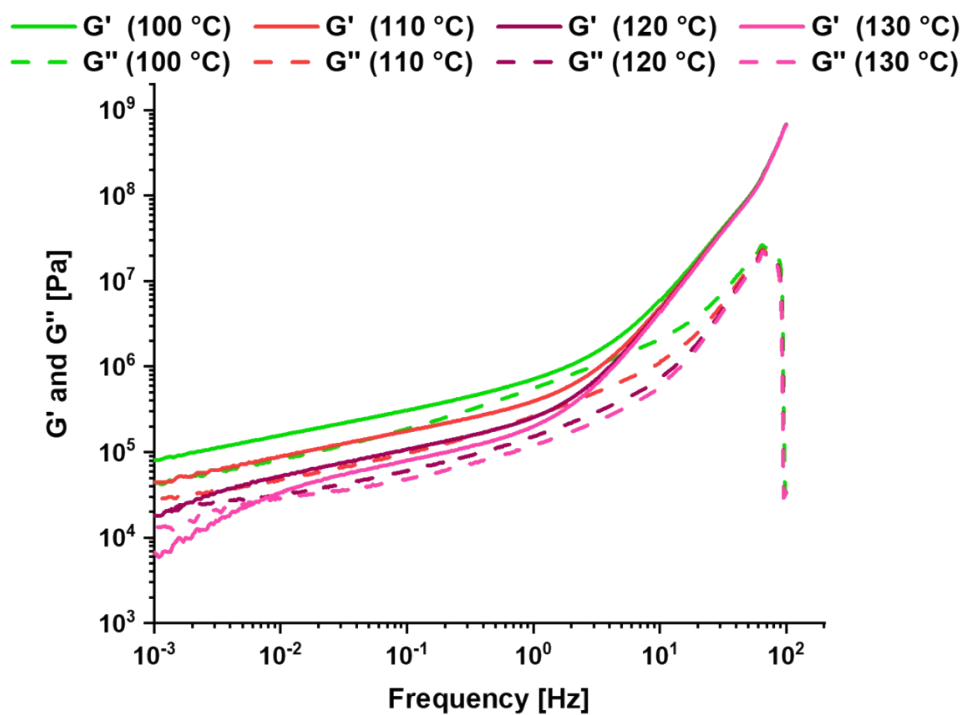


Figure S19. Frequency sweep DMA of the metallopolymer network **P2-Fe/Ni** at different temperatures (100 °C (green); 110 °C (orange); 120 °C (dark red); 130 °C (pink)).

Supporting Information

Table S7. Summary of the performed frequency sweep measurements with the metallopolymer networks **P1-Fe/Zn**, **P2-Fe/Zn**, **P1-Ni/Zn**, **P2-Ni/Zn**, **P1-Fe/Ni** and **P2-Fe/Ni** at different temperatures.

Metallopolymer	Temperature [°C]	Shear strain [%]	Crossover [Hz]	Calculated supramolecular bond lifetime [s]
P1-Fe/Zn	90	0.05	-	-
	100	0.05	-	-
	110	0.05	0.005	209
	120	0.05	0.015	69
P2-Fe/Zn	80	0.05	-	-
	90	0.05	-	-
	100	0.05	-	-
	110	0.05	0.001	983
	120	0.05	0.004	251
	130	0.05	0.011	89
P1-Ni/Zn	80	0.01	-	-
	90	0.01	0.002	575
	100	0.05	0.013	76
	110	0.01	0.102	9.8
	120	0.05	0.427	2.3
P2-Ni/Zn	80	0.01	-	-
	90	0.01	0.001	794
	100	0.05	0.012	81
	110	0.01	0.028	35
	120	0.05	0.066	15
P1-Fe/Ni	70	0.01	-	-
	85	0.1	-	-
	90	0.05	-	-
	100	0.1	0.002	549
	110	0.05	0.015	68
P2-Fe/Ni	80	0.1	-	-
	90	0.1	-	-
	100	0.1	-	-
	110	0.1	-	-
	120	0.1	0.001	725
	130	0.1	0.007	134

Thermo mechanical analysis

The thermo mechanical analysis was performed to calculate the fixity (R_f) and recovery rates (R_r) of the metallopolymer networks following **Equations S2** and **S3**. After fixing the sample into the rheometer, the temperature was set to the switching temperature (T_{sw}). The metallopolymer network in its determined permanent shape (γ_A) was deformed at this temperature ($\gamma_{B, prog.}$) (tuning in linear ramp) until the shear stress reached the shear stress value, which corresponds to a deformation of about 120° (this value was detected in a prior measurement at the same temperature). Subsequently, the sample was cooled to 25°C (10 K min^{-1}) under constant shear stress to fix the temporary shape. Thereafter, the release of the shear stress (to 0 Pa) was performed (γ_B). For the recovery process, the sample was heated again to the initial temperature (15 K min^{-1}) followed by an annealing step at this temperature leading to the recovery of the permanent shape ($\gamma_{A, rec.}$). The measurement was in general repeated three times without interruptions.

$$R_f = \gamma_B / \gamma_{B, prog.} \times 100\% \quad (\text{S2})$$

$$R_r = (\gamma_{B, prog.} - \gamma_{A, rec.}) / (\gamma_{B, prog.} - \gamma_A) \times 100\% \quad (\text{S3})$$

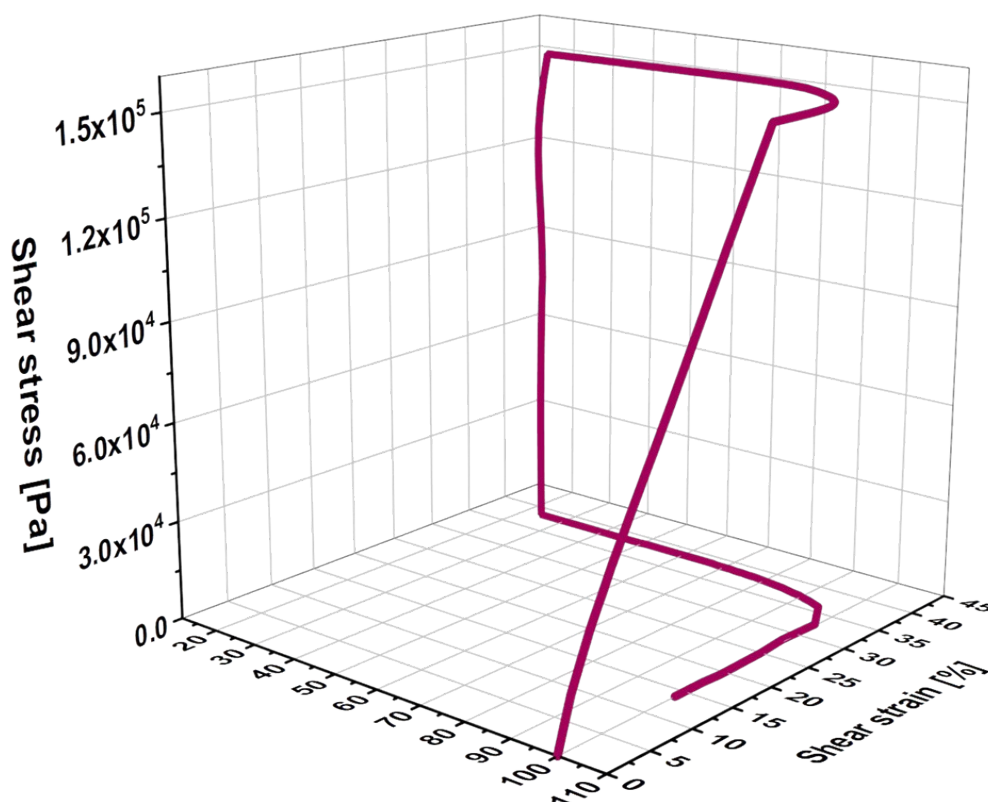


Figure S20. Plot of the thermo mechanical analysis of the metallopolymer network **P1-Fe/Zn** at a switching temperature of 100°C (first cycle).

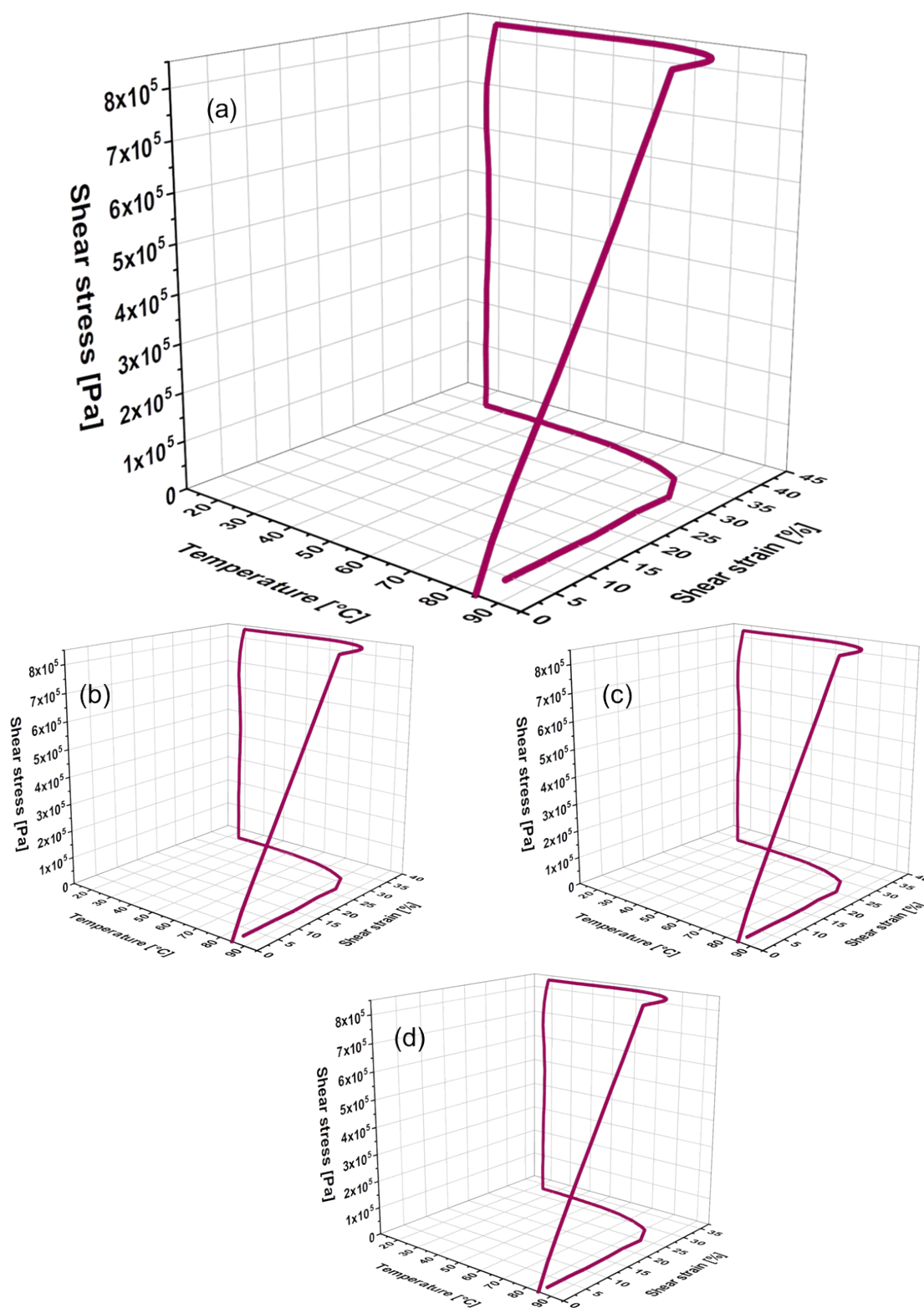


Figure S21. Plots of the thermo mechanical analysis of the metallopolymer network **P1-Fe/Zn** at a switching temperature of 90 °C (cycles: first (a), second (b), third (c) and fourth (d)).

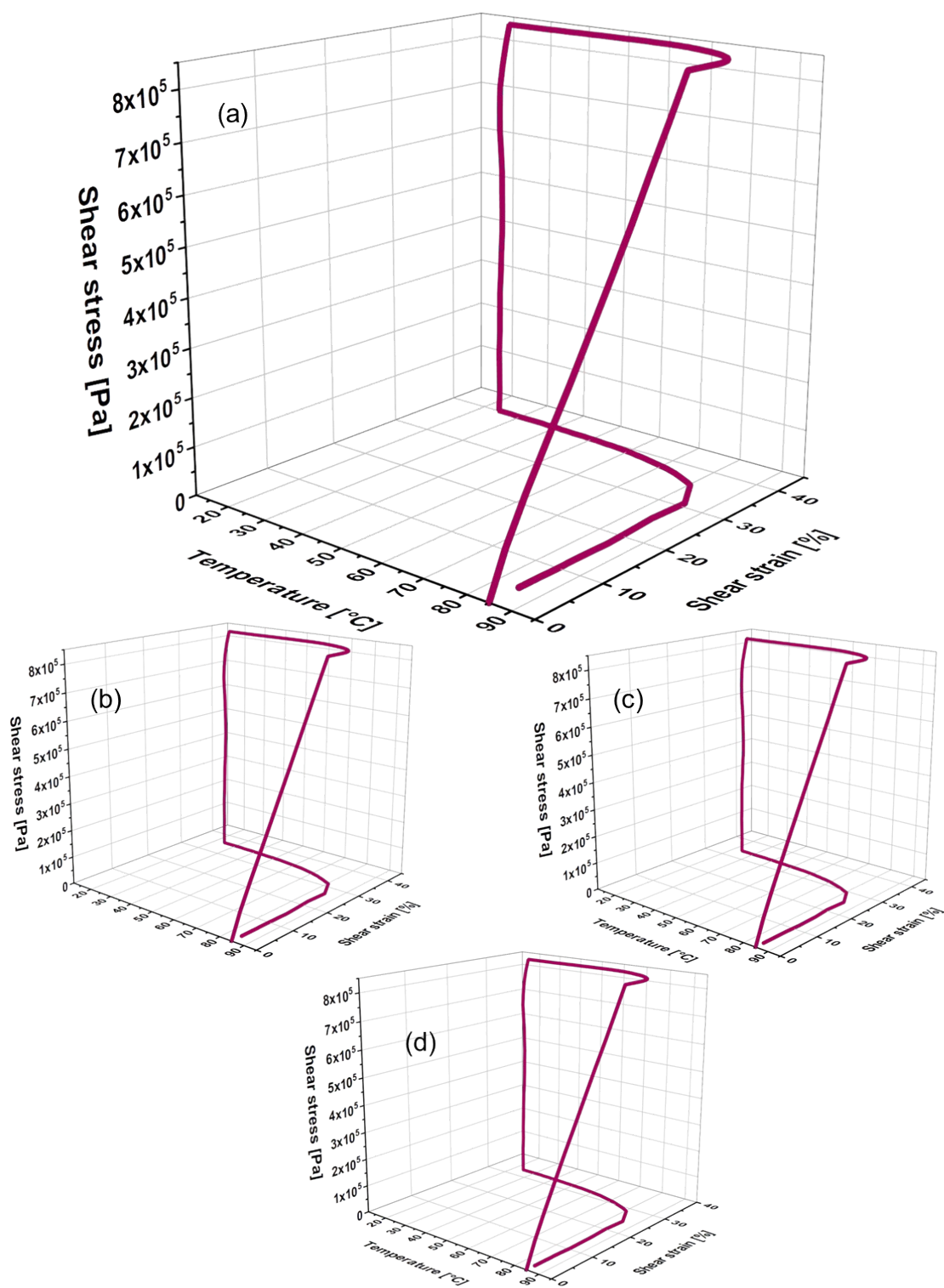


Figure S22. Plots of the thermo mechanical analysis of the metallopolymer network **P1-Fe/Zn** at a switching temperature of 85 °C (cycles: first (a), second (b), third (c) and fourth (d)).

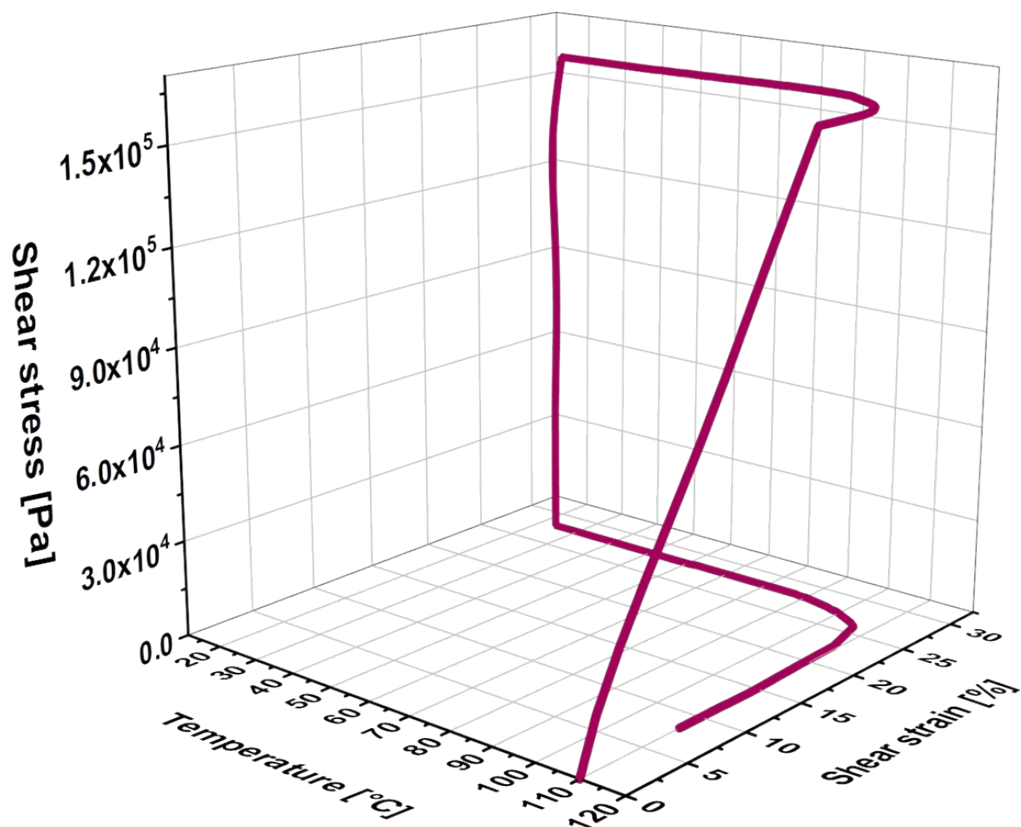


Figure S23. Plot of the thermo mechanical analysis of the metallopolymer network **P2-Fe/Zn** at a switching temperature of 110 °C (first cycle).

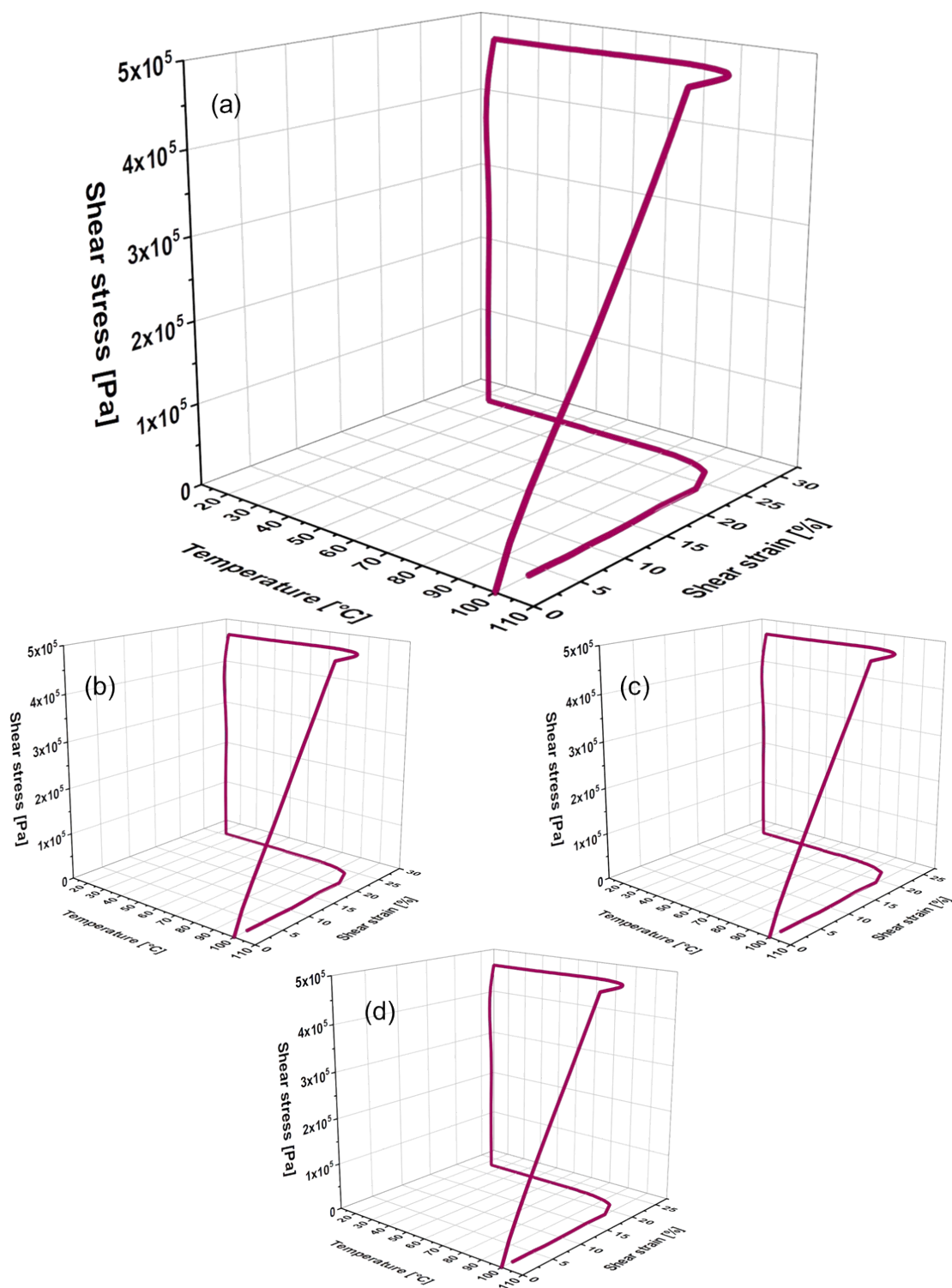


Figure S24. Plots of the thermo mechanical analysis of the metallopolymer network **P2-Fe/Zn** at a switching temperature of 100 °C (cycles: first (a), second (b), third (c) and fourth (d)).

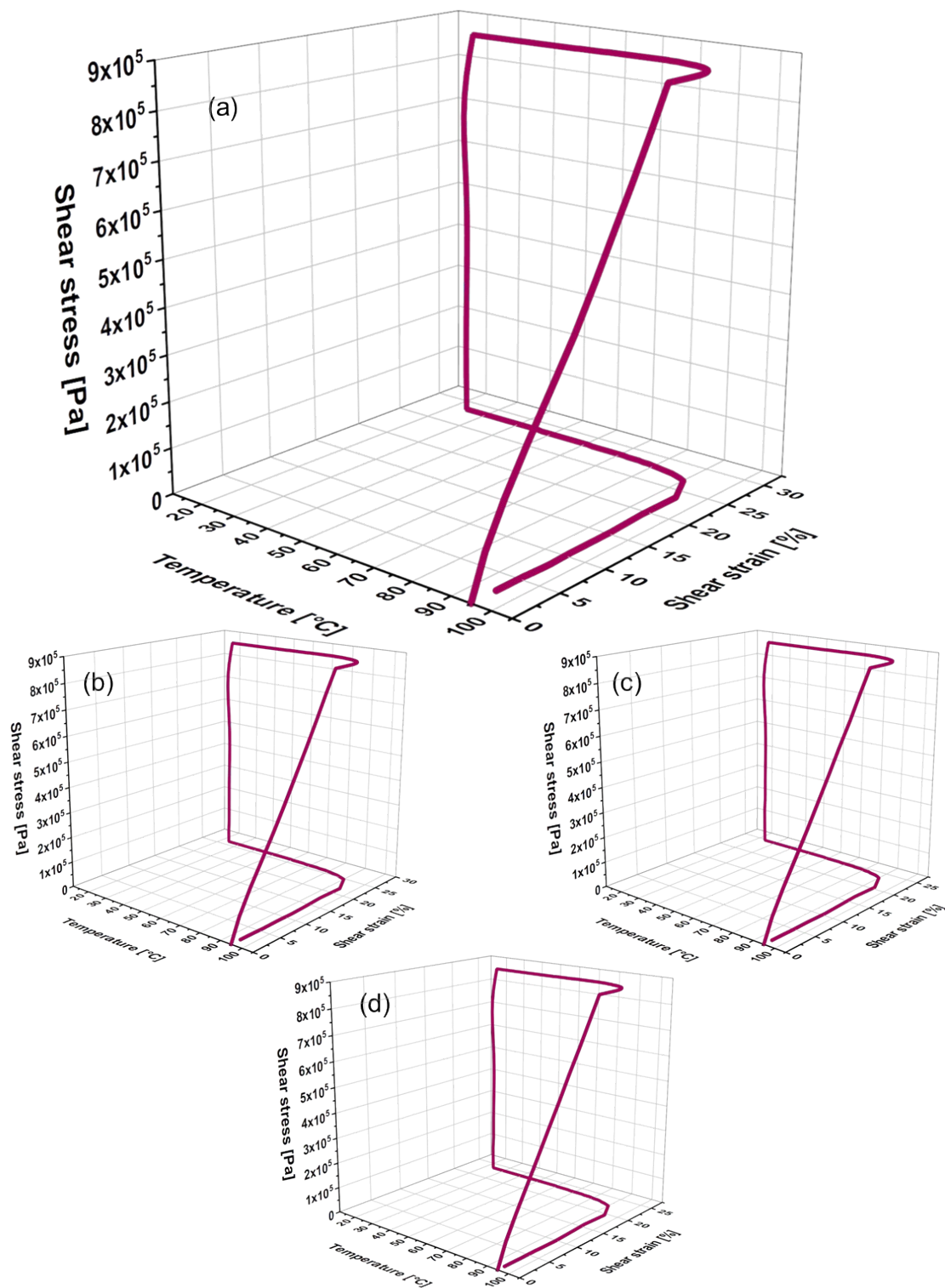


Figure S25. Plots of the thermo mechanical analysis of the metallopolymer network **P2-Fe/Zn** at a switching temperature of 95 °C (cycles: first (a), second (b), third (c) and fourth (d)).

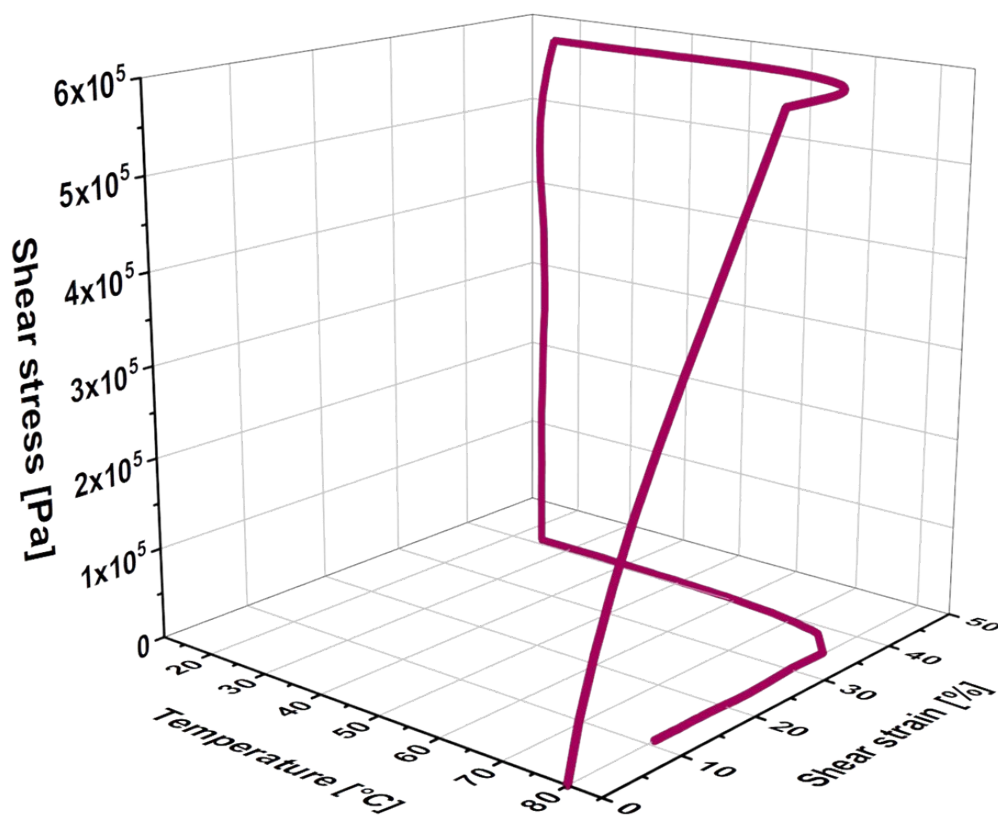


Figure S26. Plot of the thermo mechanical analysis of the metallopolymer network **P1-Ni/Zn** at a switching temperature of 80 °C (first cycle).

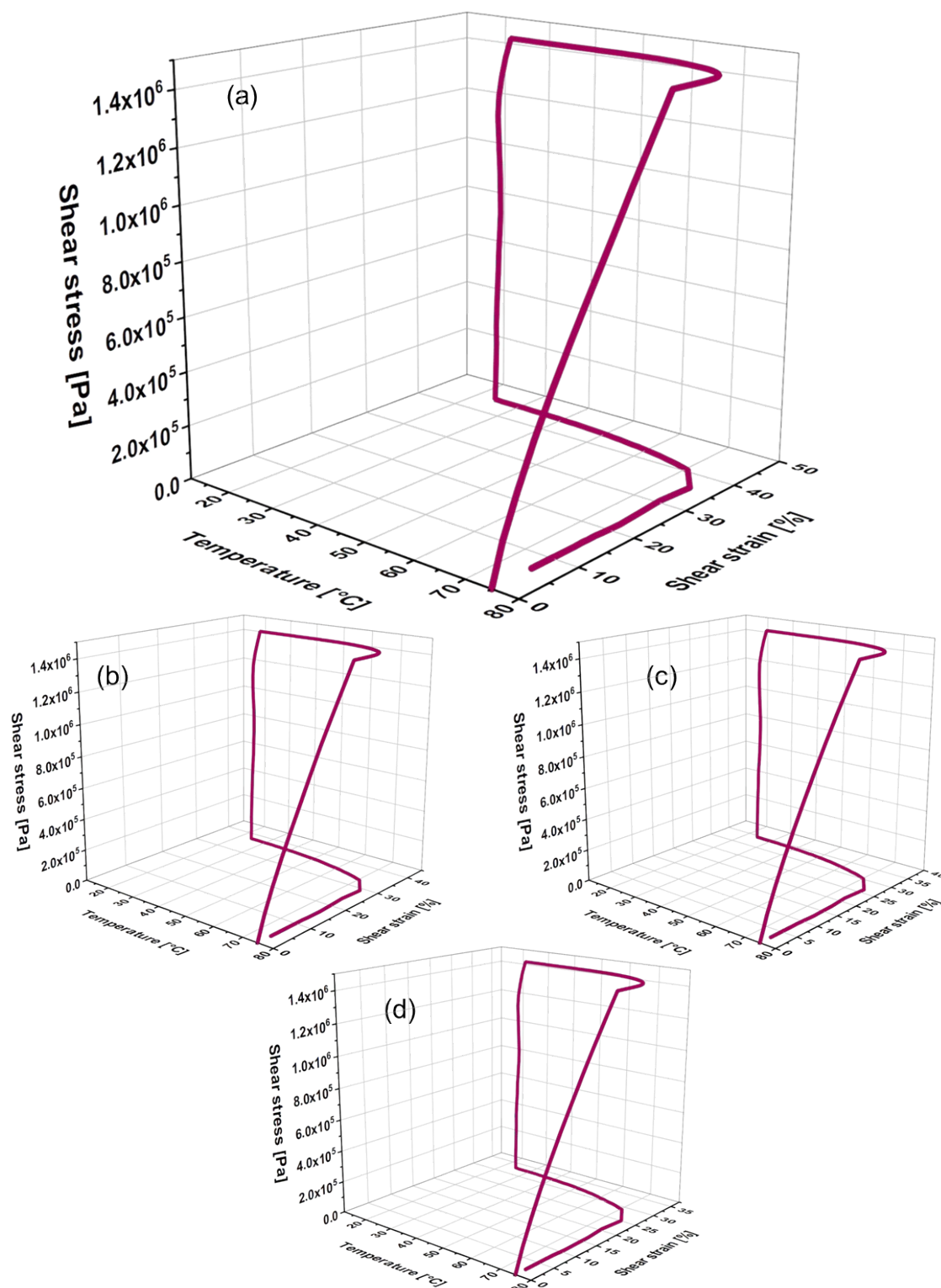


Figure S27. Plots of the thermo mechanical analysis of the metallopolymer network **P1-Ni/Zn** at a switching temperature of 75 °C (cycles: first (a), second (b), third (c) and fourth (d)).

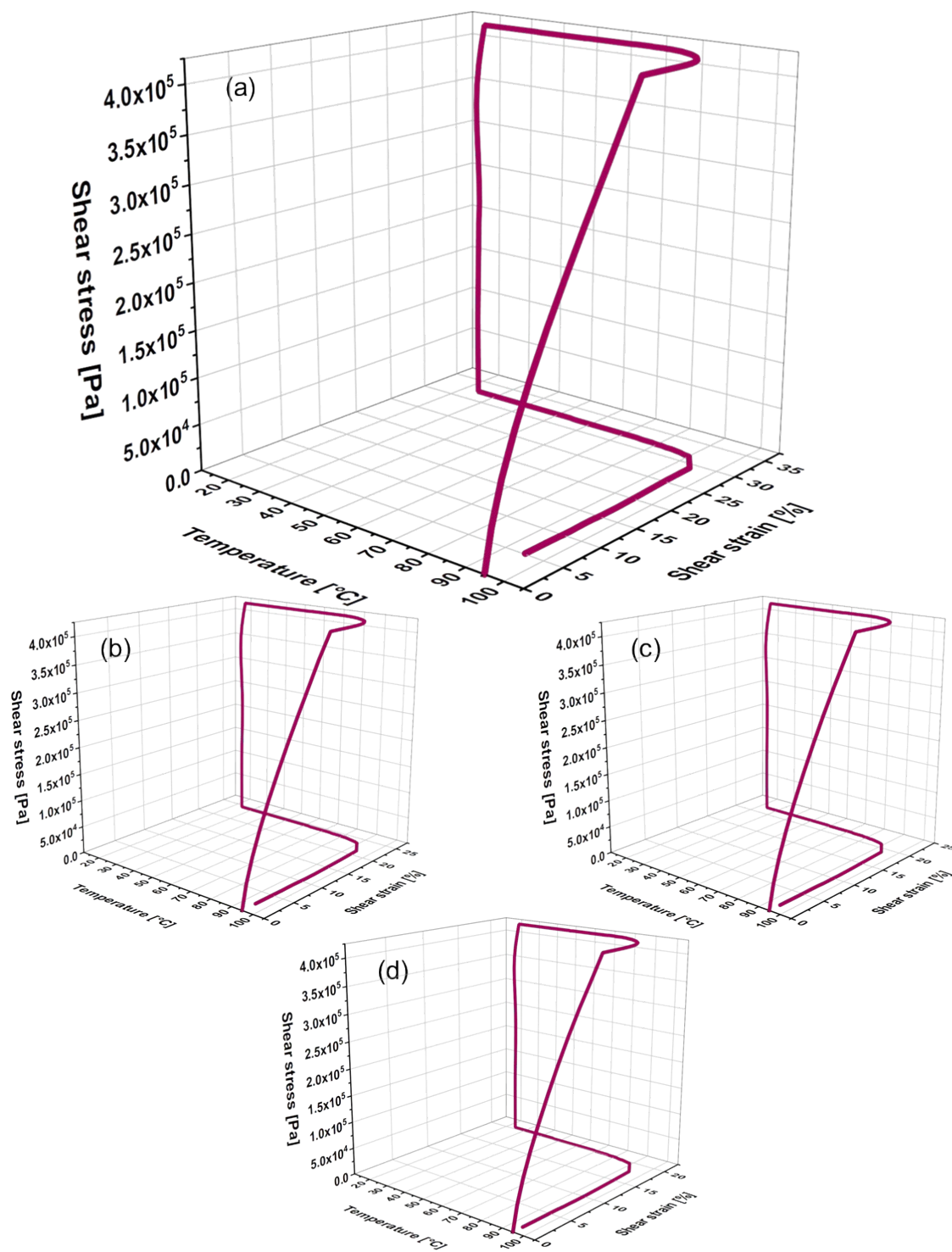


Figure S28. Plots of the thermo mechanical analysis of the metallopolymer network **P2-Ni/Zn** at a switching temperature of 95 °C (cycles: first (a), second (b), third (c) and fourth (d)).

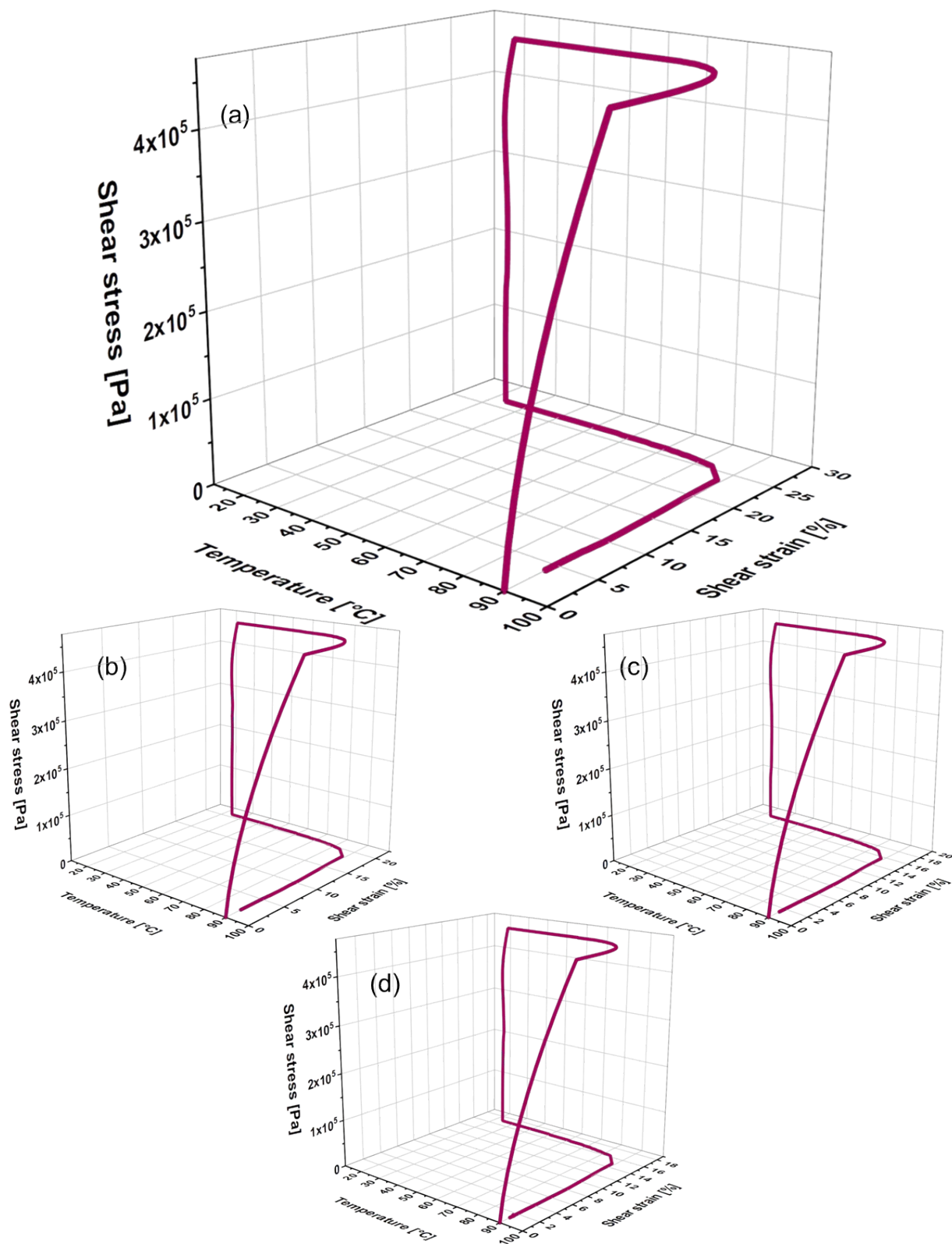


Figure S29. Plots of the thermo mechanical analysis of the metallopolymer network **P2-Ni/Zn** at a switching temperature of 90 °C (cycles: first (a), second (b), third (c) and fourth (d)).

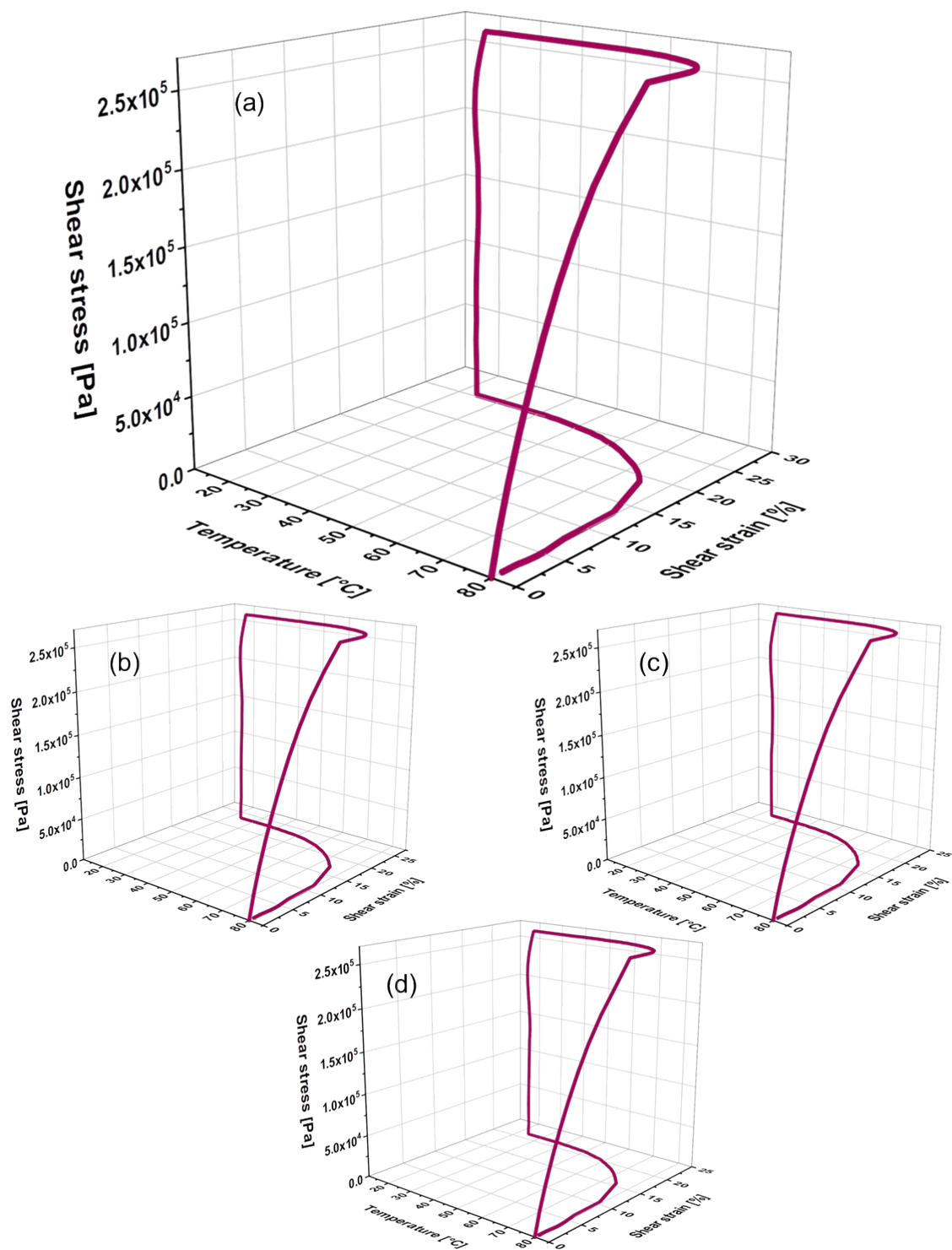


Figure S30. Plots of the thermo mechanical analysis of the metallopolymer network P1-Fe/Ni at a switching temperature of 80 °C (cycles: first (a), second (b), third (c) and fourth (d)).

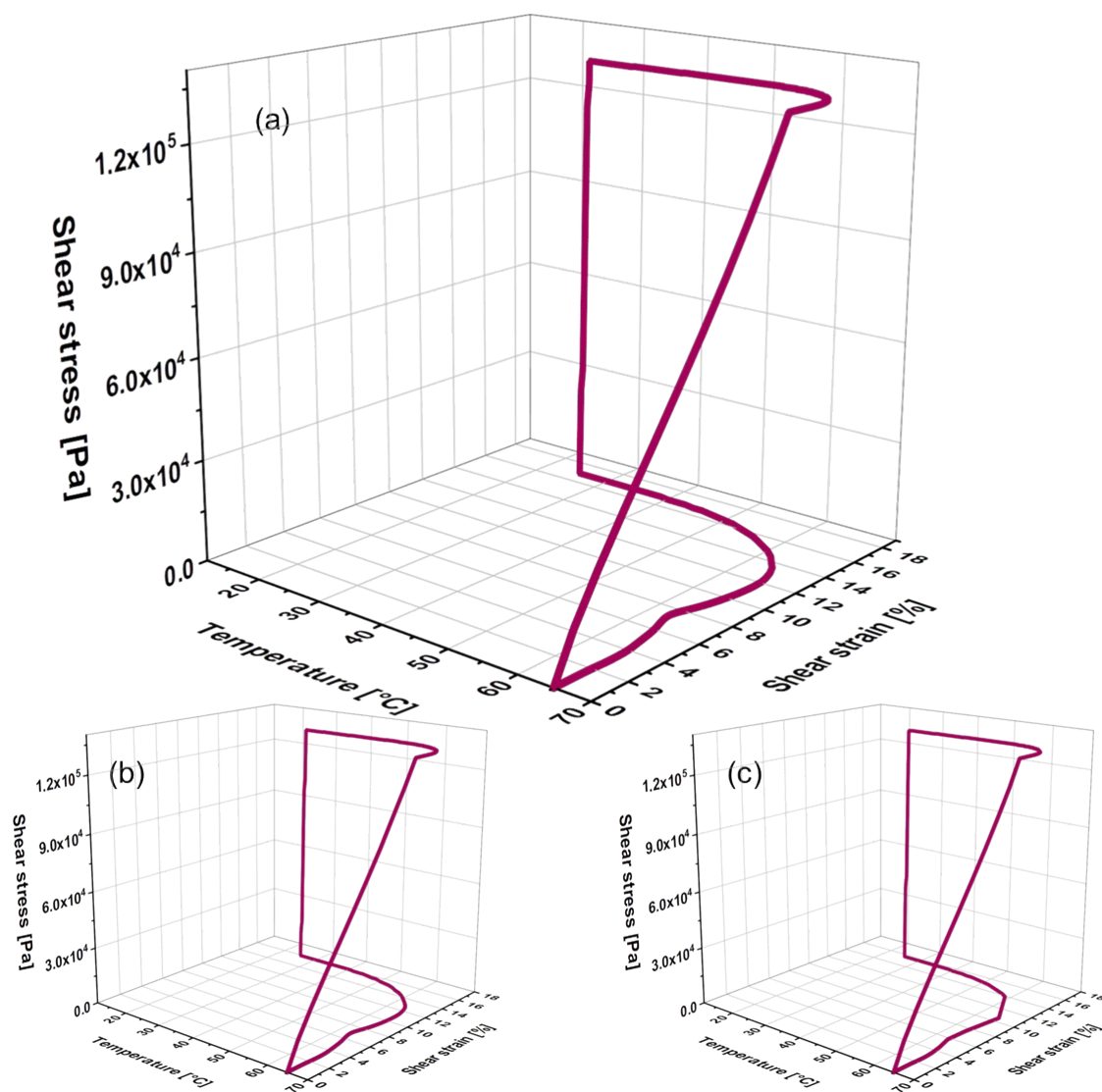


Figure S31. Plots of the thermo mechanical analysis of the metallopolymer network **P1-Fe/Ni** at a switching temperature of 65 °C (cycles: first (a), second (b) and third (c)).

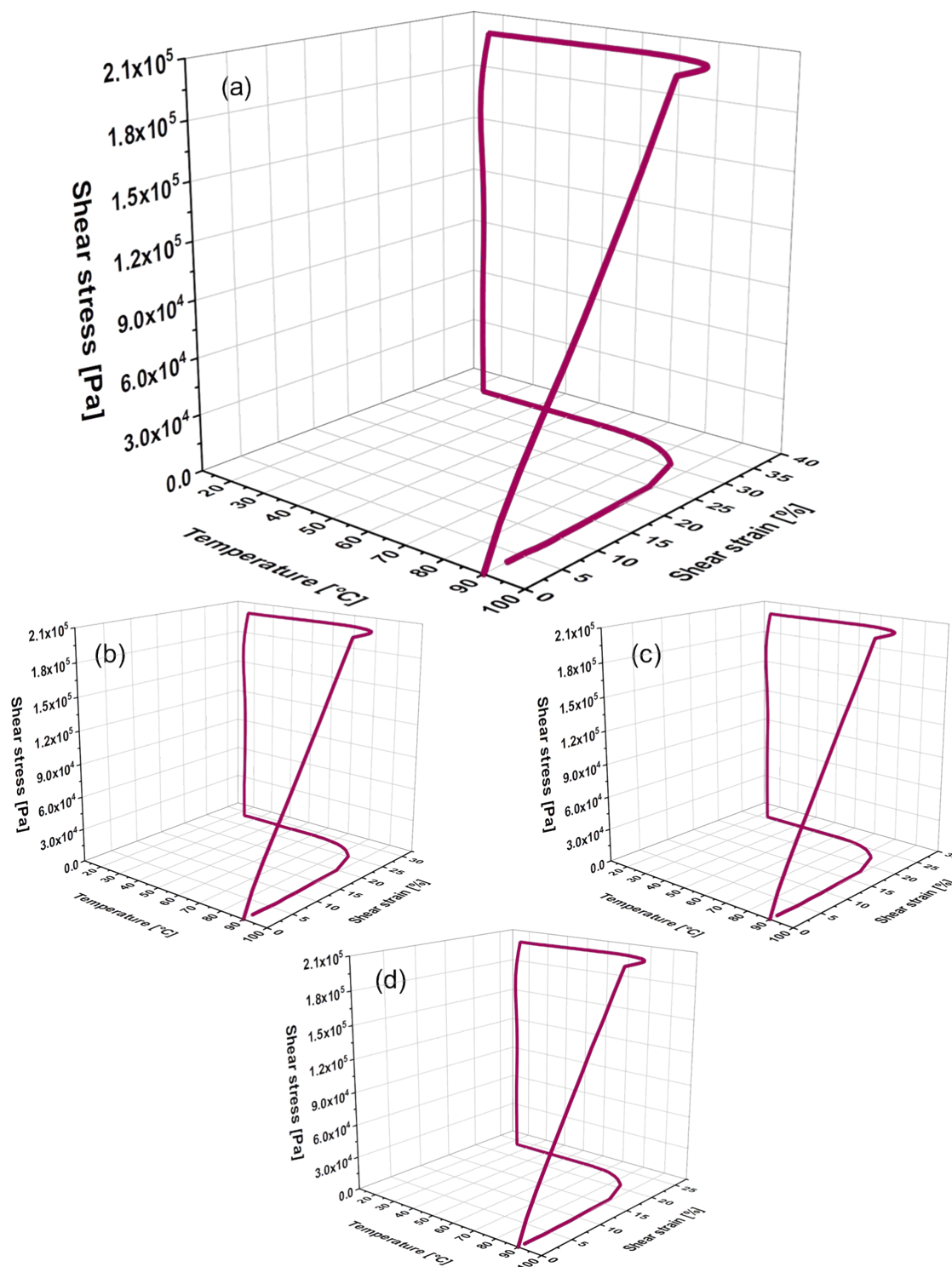


Figure S32. Plots of the thermo mechanical analysis of the metallopolymer network **P2-Fe/Ni** at a switching temperature of 90 °C (cycles: first (a), second (b), third (c) and fourth (d)).

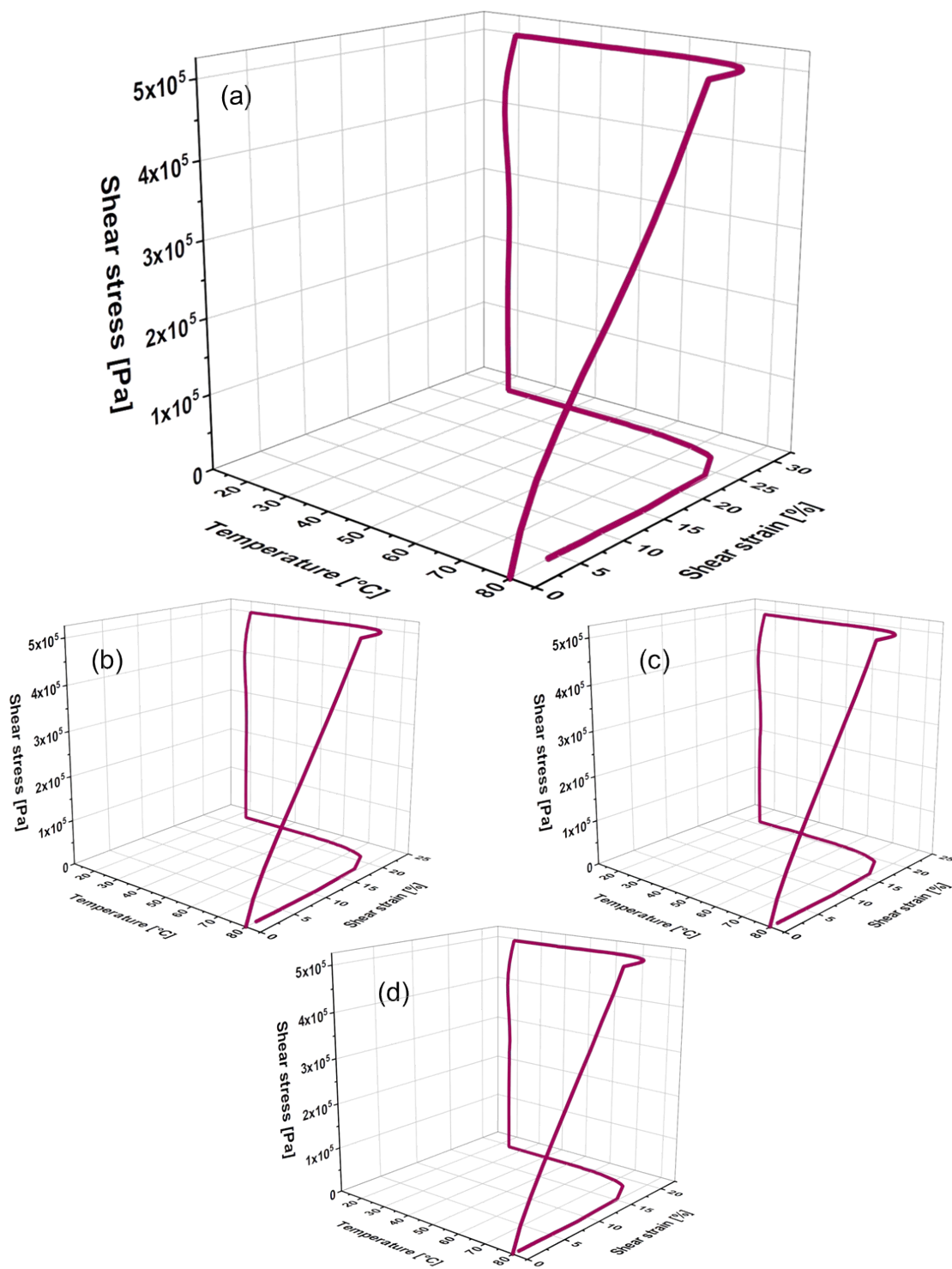


Figure S33. Plots of the thermo mechanical analysis of the metallopolymer network **P2-Fe/Ni** at a switching temperature of 80 °C (cycles: first (a), second (b), third (c) and fourth (d)).

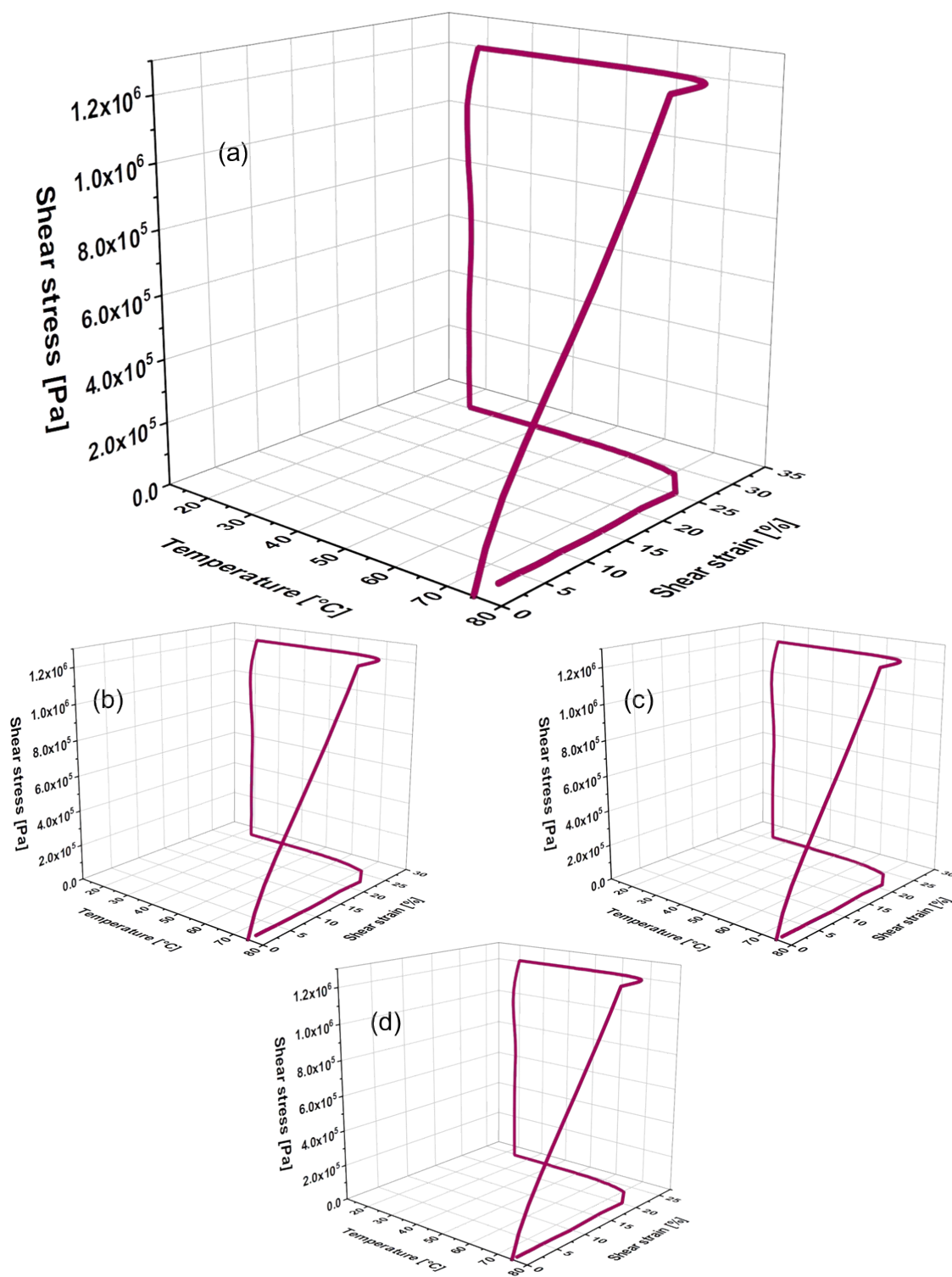


Figure S34. Plot of the thermo mechanical analysis of the metallopolymer network **P2-Fe/Ni** at a switching temperature of 75 °C (cycles: first (a), second (b), third (c) and fourth (d)).

Supporting Information

Table S8. Results of the thermo-mechanical analysis of the metallopolymer networks **P1-Fe/Zn**, **P2-Fe/Zn**, **P1-Ni/Zn**, **P2-Ni/Zn**, **P1-Fe/Ni** and **P2-Fe/Ni** at different switching temperatures.

Metallopolymer	Temp. [°C]	Cycle	γ_A [%]	$\gamma_{B, \text{prog.}}$ [%]	γ_B [%]	$\gamma_{A, \text{rec}}$ [%]	R_f [%]	R_r [%]	
P1-Fe/Zn	100	1	0	38.4	38.4	13.8	97.5	65.0	
		4	0	33.0	33.0	2.9	97.3	91.4	
	90	1	0	42.3	41.3	6.2	97.6	85.3	
		2	0	37.1	36.1	3.8	97.3	89.8	
		3	0	35.2	34.3	3.3	97.4	90.6	
		4	0	33.9	33.0	2.9	97.3	91.4	
	85	1	0	41.2	40.1	4.3	97.3	89.6	
		2	0	36.9	35.9	2.6	97.3	93.0	
		3	0	34.9	33.9	2.1	97.1	94.0	
		4	0	34.1	33.1	1.9	97.1	94.4	
	P2-Fe/Zn	110	1	0	28.6	28.0	8.2	97.9	71.3
			4	0	22.8	22.8	1.8	98.3	92.2
100		1	0	29.0	28.6	3.6	98.6	87.6	
		2	0	25.8	25.4	2.3	98.4	91.1	
		3	0	24.0	23.7	1.8	98.8	92.5	
		4	0	23.2	22.8	1.8	98.3	92.2	
95		1	0	28.6	28.4	2.6	99.3	90.9	
		2	0	26.5	26.2	1.7	98.9	93.6	
		3	0	25.0	24.7	1.3	98.8	94.8	
		4	0	23.9	23.6	1.1	98.7	95.4	
P1-Ni/Zn		80	1	0	41.9	41.1	13.0	98.1	69.0
			4	0	33.0	33.0	2.2	96.8	93.5
	75	1	0	45.9	44.7	6.6	97.4	85.6	
		2	0	38.7	37.5	3.4	96.9	91.3	
		3	0	35.4	34.4	2.5	97.2	92.9	
		4	0	34.1	33.0	2.2	96.8	93.5	
	P2-Ni/Zn	95	1	0	32.5	32.3	5.1	99.4	84.3
			2	0	24.5	24.4	2.2	99.6	91.0
3			0	21.9	21.8	1.6	99.5	92.7	
4			0	20.5	20.4	1.3	99.5	93.7	
90		1	0	26.5	26.4	4.0	99.6	84.9	
		2	0	20.8	20.7	2.0	99.5	90.4	
		3	0	17.9	17.8	1.3	99.4	92.7	
		4	0	17.1	17.0	1.1	99.4	93.6	
P1-Fe/Ni	80	1	0	25.6	25.3	1.1	98.8	95.7	
		2	0	23.6	23.2	0.8	98.3	96.6	
		3	0	22.6	22.3	0.7	98.7	96.9	
		4	0	21.8	21.4	0.7	98.2	96.8	
	65	1	0	17.3	16.9	0.4	97.7	97.7	
		3	0	16.0	15.6	0.2	97.5	98.8	
P2-Fe/Ni	90	1	0	35.4	34.8	3.1	98.3	91.2	
		2	0	29.1	28.5	1.7	97.9	94.2	
		3	0	26.2	25.6	1.3	97.7	95.0	
		4	0	24.3	23.7	1.0	97.5	95.9	
	80	1	0	29.4	29.1	4.2	99.0	85.7	
		2	0	22.8	22.6	1.5	99.1	93.4	
		3	0	21.0	20.7	1.1	98.6	94.8	
		4	0	19.9	19.6	0.8	98.5	96.0	
	75	1	0	30.4	30.2	2.8	99.3	90.8	
		2	0	27.4	27.2	1.4	99.3	94.9	
		3	0	25.8	25.7	1.0	99.6	96.1	
		4	0	24.8	24.7	0.8	99.6	96.8	

Rewriting investigation

To rewrite the permanent shape of a previously hot pressed metallopolymer network (rectangular shape), the sample was fixed in the rheometer. The temperature was set to 110 °C. After annealing, the sample was turned about 180°. This led to a rise of the shear strain caused by the deformation (see **Figure S40**). The deformation and temperature were kept constant, leading to a decrease of the shear strain (nearly 0 Pa) caused by the rewriting of the permanent shape.

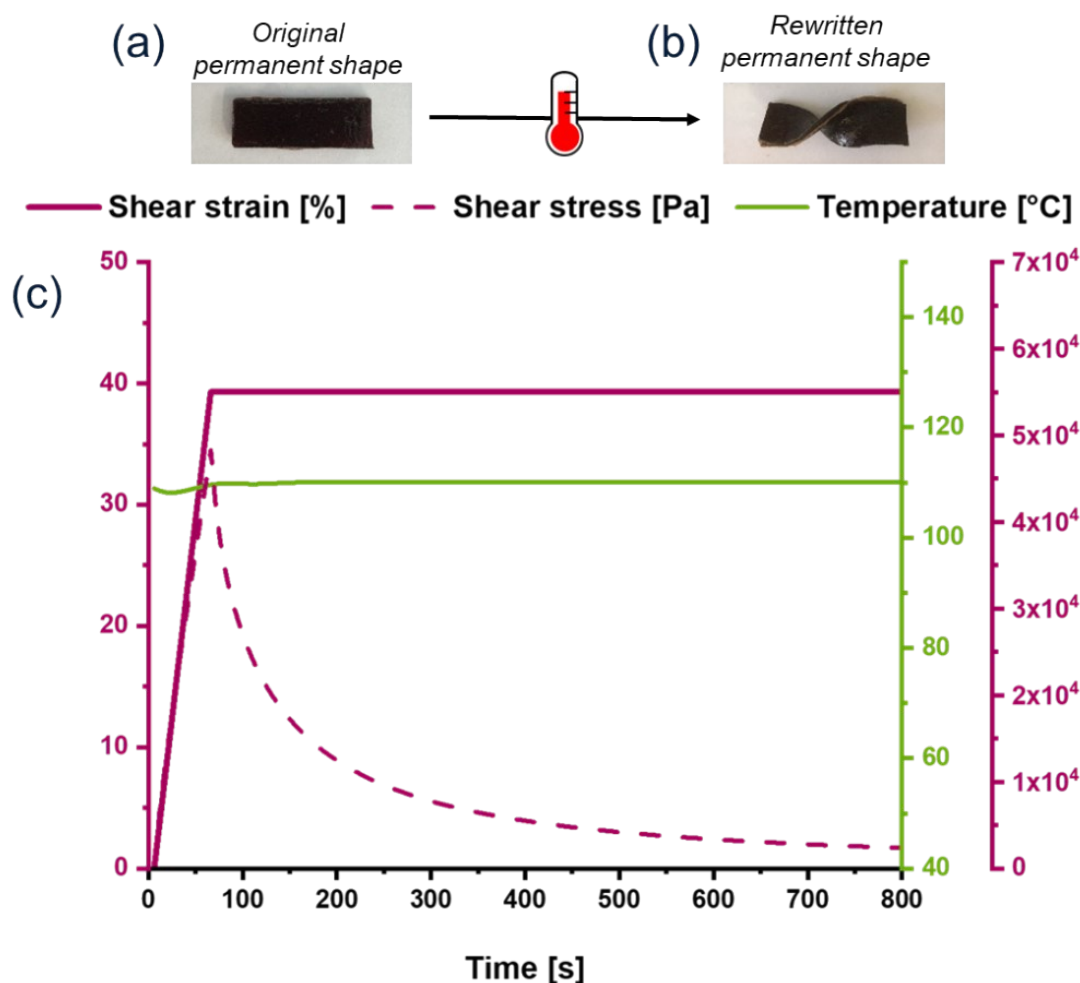


Figure S35. Rewriting of the metallopolymer network **P2-Fe/Ni** (a: Photo of the determined permanent shape after hot pressing. b: Rewritten permanent shape in the rheometer, c: Plot of the rewriting).

Furthermore, thermo mechanical analyses were performed to investigate the influence of the rewriting on the shape memory abilities of the metallopolymer networks. The fixity (R_f) and recovery rates (R_r) of the metallopolymer networks were calculated according to **Equations S2** and **S3** before and after the rewriting. In the first steps of this investigation a standard TMA was performed. After fixing the sample into the rheometer, the temperature was set to the switching temperature (T_{sw}). The metallopolymer network in its determined permanent shape (γ_A) was deformed at this temperature ($\gamma_{B, prog.}$) (tuning in linear ramp) until the shear stress reached the shear stress value, which corresponds

to a deformation of about 120° (this value was detected in a prior measurement at the same temperature). Subsequently, the sample was cooled to 25 °C (10 to 2 K min⁻¹) under constant shear stress to fix the temporary shape. Thereafter, the release of the shear stress (to 0 Pa) was performed (γ_B). For the recovery process, the sample was heated again to the initial temperature (15 K min⁻¹) followed by an annealing step at this temperature leading to the recovery of the permanent shape ($\gamma_{A, rec.}$). Afterwards, to rewrite the permanent shape, the sample was heated to 110 °C, and turned about 120° ($\gamma_{A2, prog.}$), followed by an annealing step at this temperature (1 h) while the deformation was kept constant. Afterwards, the sample was again cooled to the switching temperature and the stress was removed from the sample (γ_{A2}). After this rewriting step, again a TMA measurement was performed. The metallopolymer network in its rewritten permanent shape (γ_{A2}) was deformed at this temperature ($\gamma_{B2, prog.}$) (tuning in linear ramp) until the shear stress reached the shear stress value, which corresponds to a deformation of about 120° (same value like first TMA). Subsequently, the sample was cooled to 25 °C (10 to 2 K min⁻¹) under constant shear stress to fix the temporary shape. Thereafter, the release of the shear stress (to 0 Pa) was performed (γ_{B2}). For the recovery process, the sample was heated again to the initial temperature (15 K min⁻¹) followed by an annealing step at this temperature leading to the recovery of the rewritten permanent shape ($\gamma_{A2, rec.}$). This measurement was performed with all metallopolymer networks. The results are summarized in **Table S9**.

Table S9. Results of the thermo-mechanical analysis of the metallopolymer networks **P1-Fe/Zn**, **P2-Fe/Zn**, **P1-Ni/Zn**, **P2-Ni/Zn**, **P1-Fe/Ni** and **P2-Fe/Ni** at different switching temperatures for the investigation of the rewriting influence.

Sample	γ_A [%]	$\gamma_{B, prog.}$ [%]	γ_B [%]	$\gamma_{A, rec.}$ [%]	$\gamma_{A2, prog.}$ [%]	γ_{A2} [%]	$\gamma_{B2, prog.}$ [%]	γ_{B2} [%]	$\gamma_{A2, rec.}$ [%]	T_{sw} [°C]	Before rewriting		E_{re} [%] (110 °C)	After rewriting	
											R_f	R_r		R_f	R_r
											[%]	[%]	[%]	[%]	
P1-Fe/Zn	0	31.8	31.2	3.5	-26.2	-25.7	15.1	14.3	-21.3	90	98.1	89.1	98.1	98.5	89.1
P2-Fe/Zn	0	49.3	49.2	5.5	-26.8	-25.0	46.9	46.4	-16.2	100	99.8	88.9	93.7	99.0	87.7
P1-Ni/Zn	0	35.0	34.1	5.0	-19.4	-19.1	1.5	0.7	-17.0	75	97.4	85.7	98.5	95.3	89.8
P2-Ni/Zn	0	49.1	49.0	7.2	-23.7	-22.3	37.9	37.7	-12.9	95	99.8	85.4	94.1	99.3	84.4
P1-Fe/Ni	0	17.3	16.7	1.2	-12.4	-12.0	19.0	18.5	-11.0	80	96.5	93.2	96.8	97.7	96.8
P2-Fe/Ni	0	28.5	28.4	1.4	-22.7	-22.1	20.1	19.9	-20.3	75	99.6	95.1	97.5	99.5	95.7

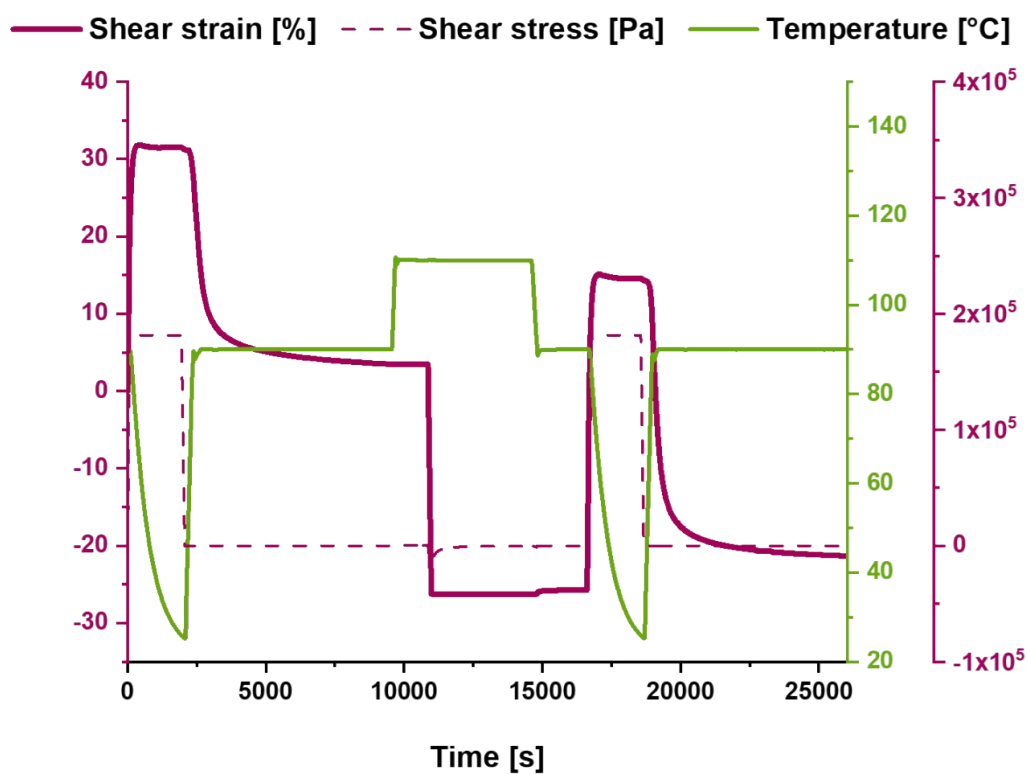


Figure S36. Plot of the thermo mechanical analysis to investigate the rewriting of the metallopolymer network P1-Fe/Zn.

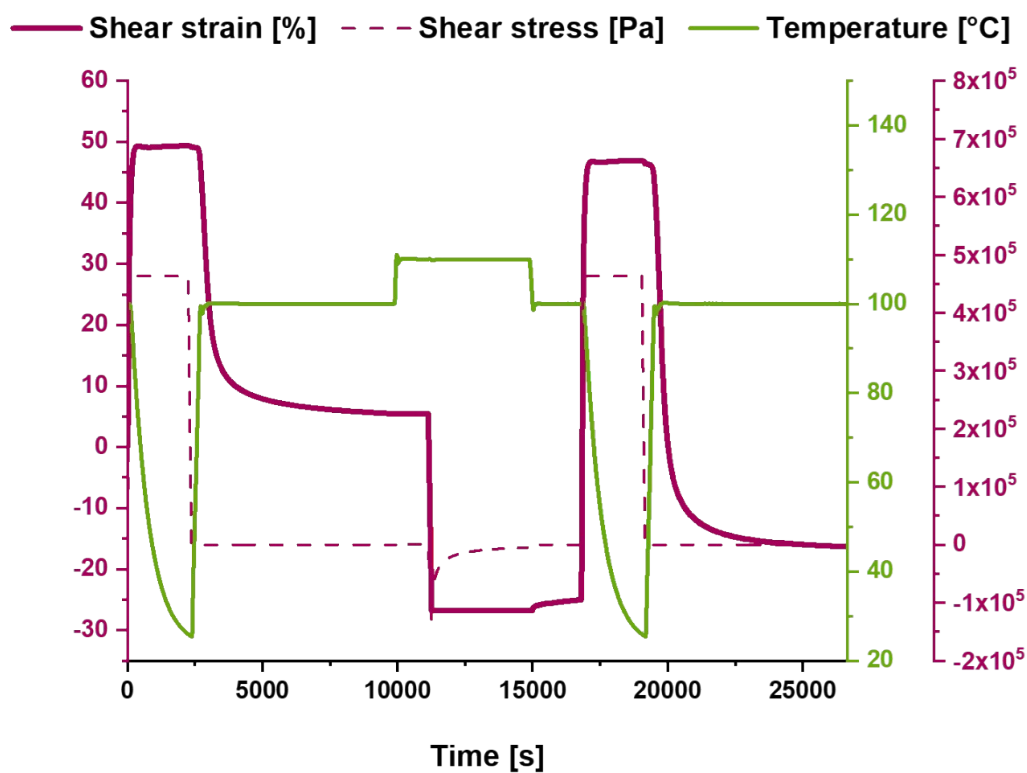


Figure S37. Plot of the thermo mechanical analysis to investigate the rewriting of the metallopolymer network P2-Fe/Zn.

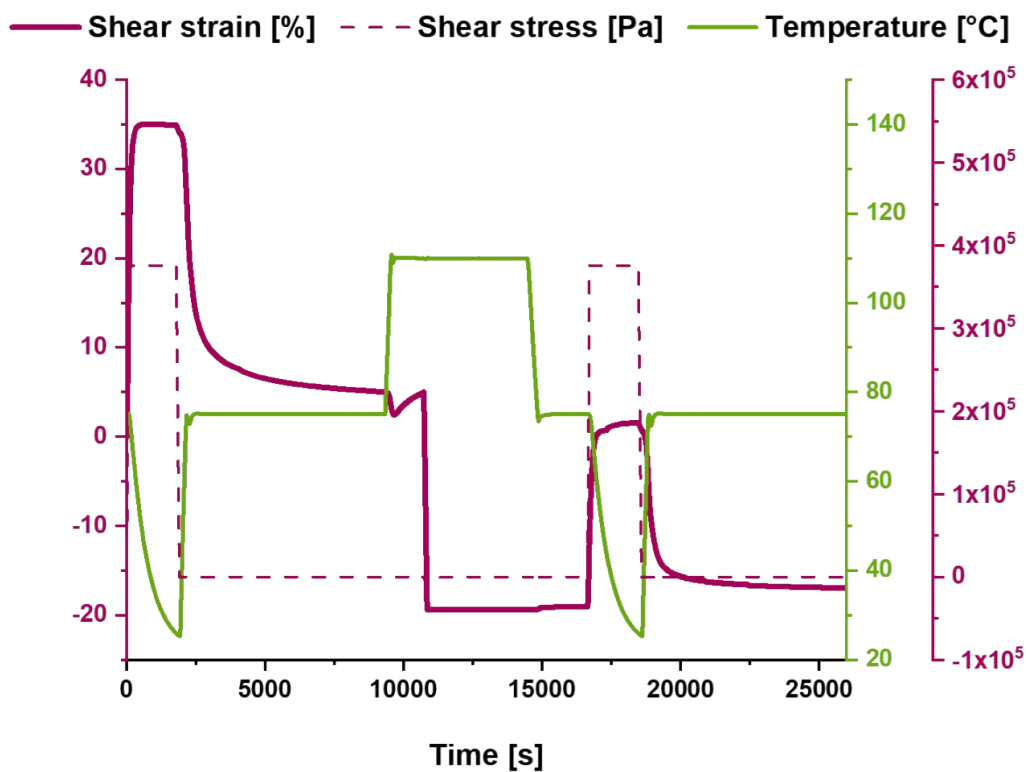


Figure S38. Plot of the thermo mechanical analysis to investigate the rewriting of the metallopolymer network P1-Ni/Zn.

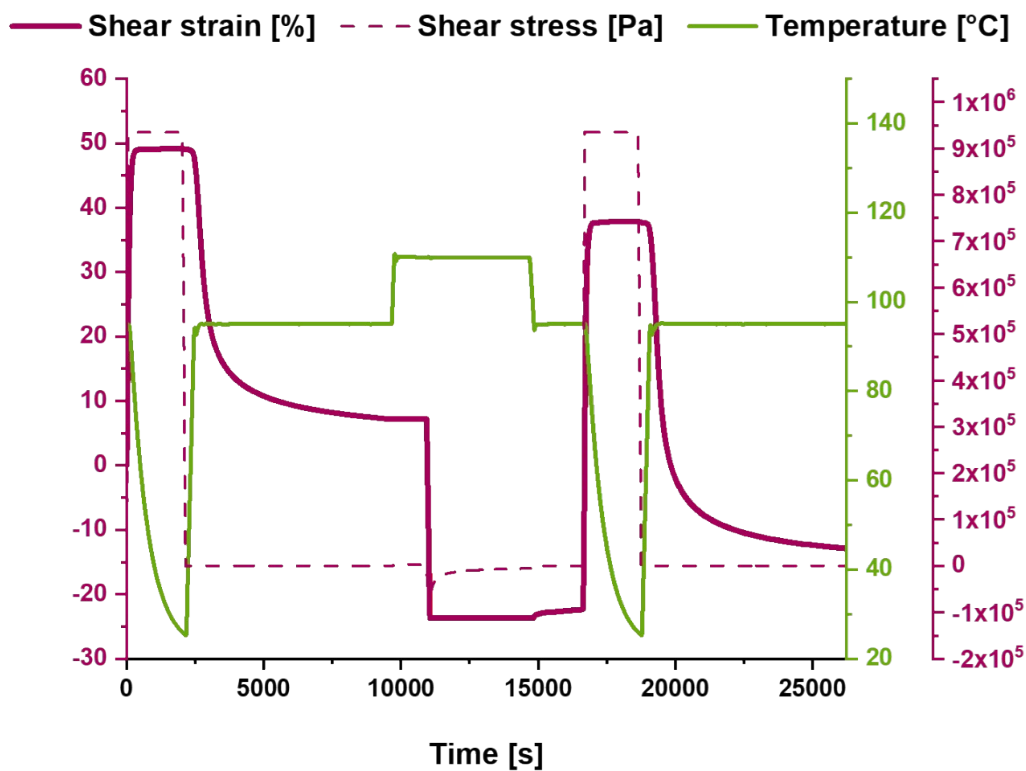


Figure S39. Plot of the thermo mechanical analysis to investigate the rewriting of the metallopolymer network P2-Ni/Zn.

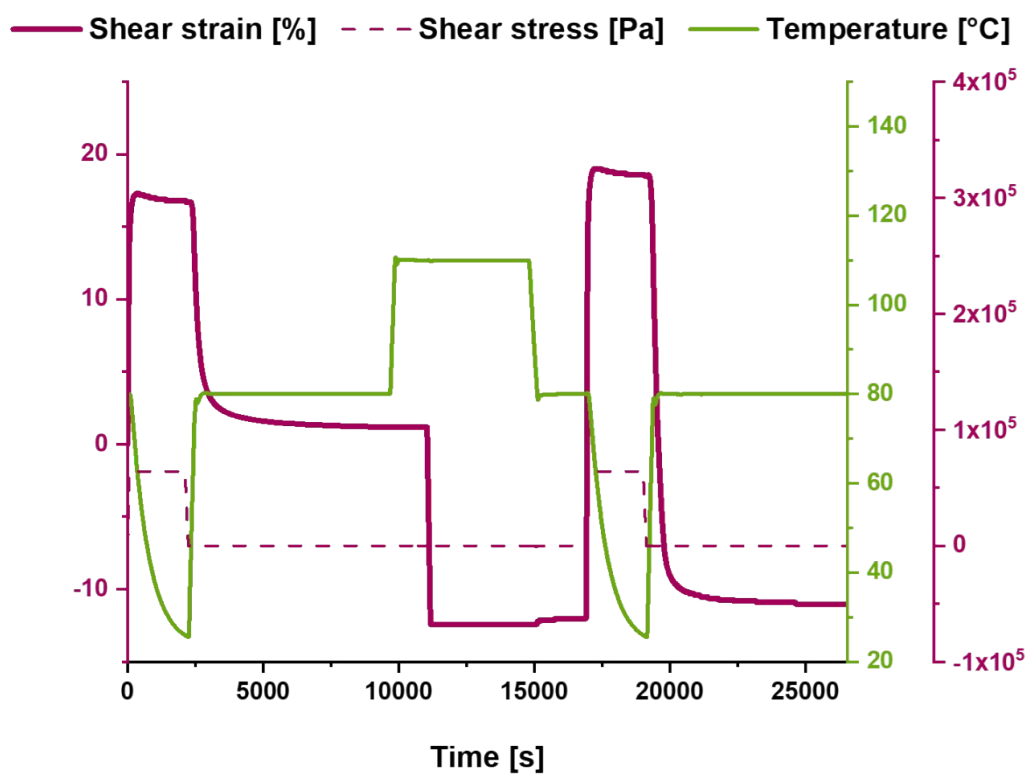


Figure S40. Plot of the thermo mechanical analysis to investigate the rewriting of the metallopolymer network P1-Fe/Ni.

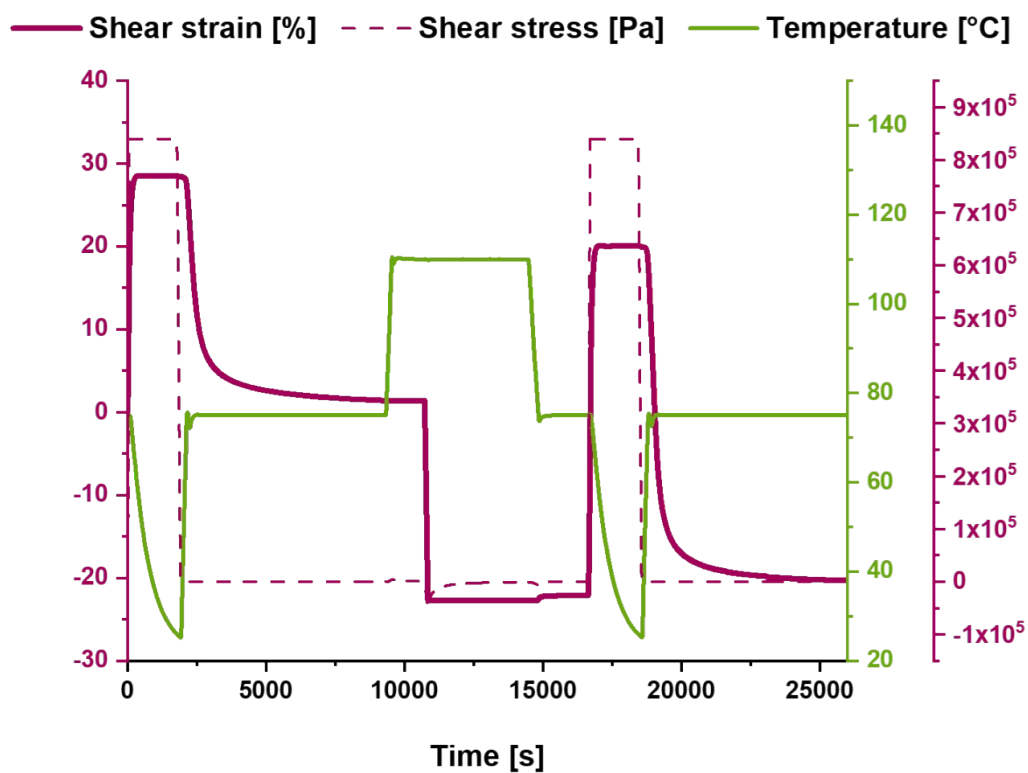


Figure S41. Plot of the thermo mechanical analysis to investigate the rewriting of the metallopolymer network P2-Fe/Ni.

Photo series of the shape-memory test

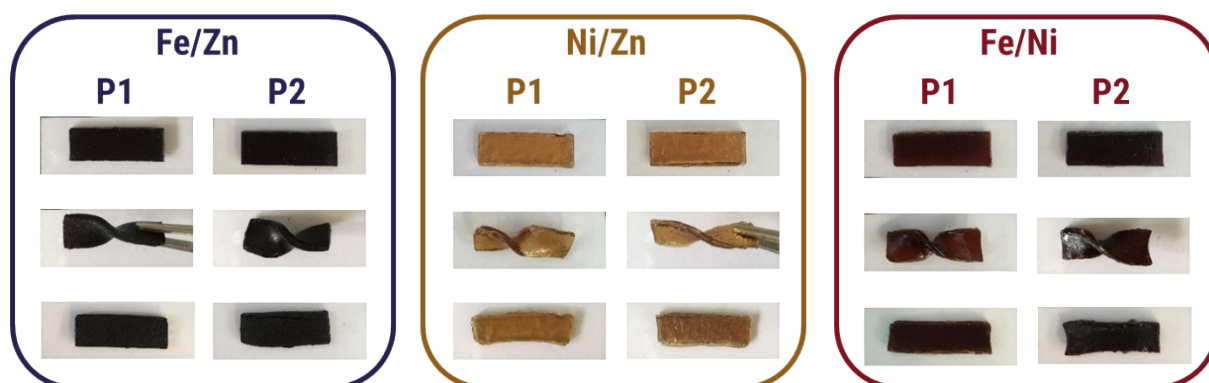


Figure S42. Photo series of the shape-memory test of the metallopolymer networks **P1-Fe/Zn** ($T_{sw} = 95\text{ }^{\circ}\text{C}$), **P2-Fe/Zn** ($T_{sw} = 110\text{ }^{\circ}\text{C}$), **P1-Ni/Zn** ($T_{sw} = 95\text{ }^{\circ}\text{C}$), **P2-Ni/Zn** ($T_{sw} = 110\text{ }^{\circ}\text{C}$), **P1-Fe/Ni** ($T_{sw} = 80\text{ }^{\circ}\text{C}$) and **P2-Fe/Ni** ($T_{sw} = 90\text{ }^{\circ}\text{C}$) (left to right) (Top: Permanent shape; middle: Fixed temporary shape; bottom: Recovered permanent shape).

FT-Raman spectroscopy

All Raman-spectroscopic measurements were performed on a Multispec Fourier-transform Raman-Spectrometer (Bruker Corporation, Billerica, Massachusetts, United States of America) in the range between 100 and 4000 cm^{-1} with a spectral resolution of 4 cm^{-1} . The Raman excitation light at 1064 nm was provided by a Nd:YAG laser (Klasech DeniCAFC-LC-3/40, Dortmund, Germany). The laser power at the sample had to be varied between 20 and 1000 mW depending on the photothermal stability of the respective sample. To improve the signal-to-noise ratio the number of accumulated scans was varied accordingly. The respective data for each sample can be found in **Table S10**.

Table S10. Laser power at sample and number of accumulated scans for the FT-Raman measurements of all samples.

Sample	Laser power (mW)	Number of scans	Sample	Laser power (mW)	Number of scans
P1	1000	256	P2	500	256
P1-Fe/Zn	20	2048	P2-Fe/Zn	20	2048
P1-Ni/Zn	500	1024	P2-Ni/Zn	20	2048
P1-Fe/Ni	20	2048	P2-Fe/Ni	20	1024
[(Tpy)₂Fe]²⁺	20	2048	[(His)₃Fe]²⁺	20	4096

For further evaluation the raw Raman data was preprocessed using R 4.0.3:⁴ The spectra were restricted to the wavenumber of interest (e.g., 700 to 1750 cm^{-1}) followed by background correction using the SNIP-algorithm (iterations: 50 , order: 3 , smoothing window: 3) and normalized using euclidean vector norm.⁵

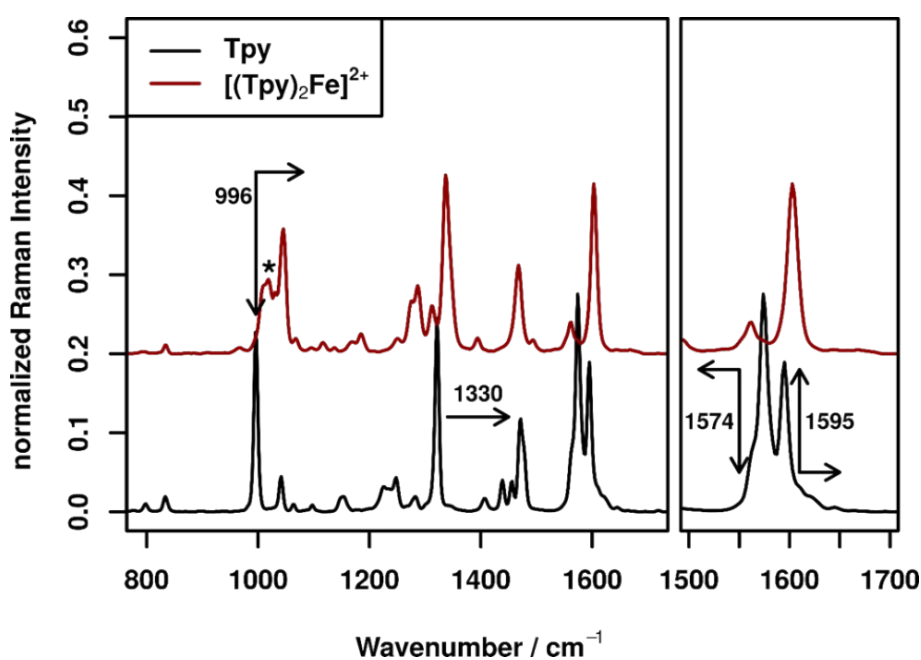
Raman-Spectra of model complexes $[(\text{Tpy})_2\text{Fe}]^{2+}$ and $[(\text{His})_3\text{Fe}]^{2+}$ 

Figure S43. Raman spectra of **Tpy** (black, bottom) and the corresponding model complex with FeSO_4 (red, top) in the wavenumber range between 800 and 1700 cm^{-1} . The arrows indicate prominent changes and their direction in the Raman spectrum upon coordination of the metal ion. Marked with a star is a band overlapped with contribution of the sulfate counterion.

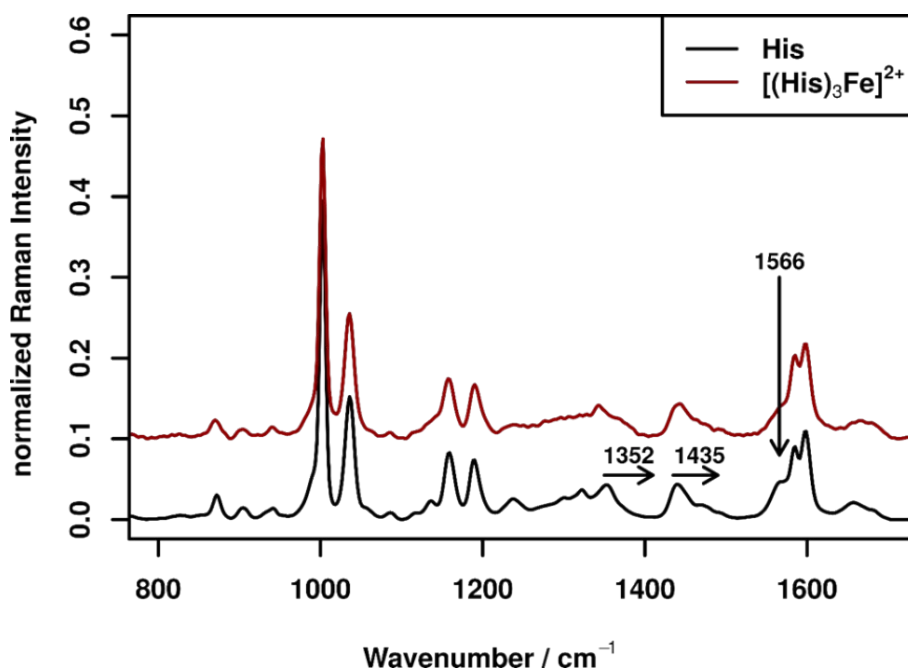


Figure S44. Raman spectra of **His** (black, bottom) and the corresponding model complex with FeSO_4 (red, top) in the wavenumber range between 800 and 1700 cm^{-1} . The arrows indicate prominent changes and their direction in the Raman spectrum upon coordination of the metal ion.

To investigate the changes that occur in the Raman spectra of **P1** and **P2** upon coordination of iron to the functional moieties, model complexes of FeSO_4 with **Tpy** and **His** were prepared and investigated with Raman spectroscopy. **Figure S43** shows the spectra of **Tpy** and **Figure S44** the spectra of **His** before and after the coordination with FeSO_4 . The coordination of the metal ion leads to noticeable changes in the Raman spectra of both model compounds, which are in particular pronounced for **Tpy**. In an earlier work,³ it has already been shown that coordination of zinc and nickel to these moieties leads to prominent changes in the Raman spectra.

For **His**, these changes are mainly caused by changes in the geometry of the moiety, which leads to changes in the bond structure of the imidazole moiety of the **His**. This leads to a strengthening of the C-N ($1352, 1435 \text{ cm}^{-1}$) and C=C (1566 cm^{-1}) bonds, which therefore shift to higher energies upon coordination.

For **Tpy** the main reason for the drastic changes in the Raman spectrum is a change from all-trans to all-cis configuration upon coordination of a metal ion. This causes significant changes in the electronic structure of the aromatic system and thereby influences the bond strengths significantly, leading to blue shifts of ca. 20 to 30 cm^{-1} for the bands at 996 cm^{-1} ($\delta\text{C-C}, \delta\text{C-N}$) and 1320 cm^{-1} ($\nu\text{C-C}$, bridging). It is therefore possible to confirm the coordination of iron to both moieties using Raman spectroscopy. The blueshifts at 1566 cm^{-1} for **Tpy** and 1352 cm^{-1} for **His** are best suited for this, since no overlap with changes caused by coordination to the other moiety occur in this case.

Comparing the changes in the Raman spectra to those caused by coordination of nickel and zinc to the moieties,³ it is further apparent that a distinction between different metal ions is not possible using Raman spectroscopy. The introduced changes on the geometry and electronic systems are very similar for all metal ions so that the corresponding differences in band positions are smaller than the natural bandwidths observed in a polymer environment.

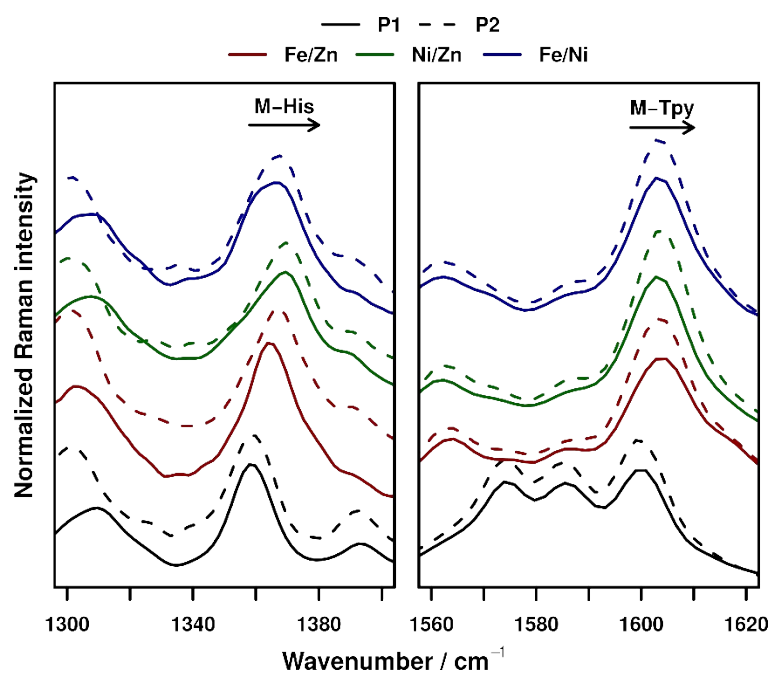


Figure S45. Raman spectra in the **His** (left) and **Tpy** (right) marker regions for the pure polymers **P1** (black, solid) and **P2** (black, dotted), and their respective metallopolymer with Fe/Zn (red), Ni/Zn (green) and Fe/Ni (blue).

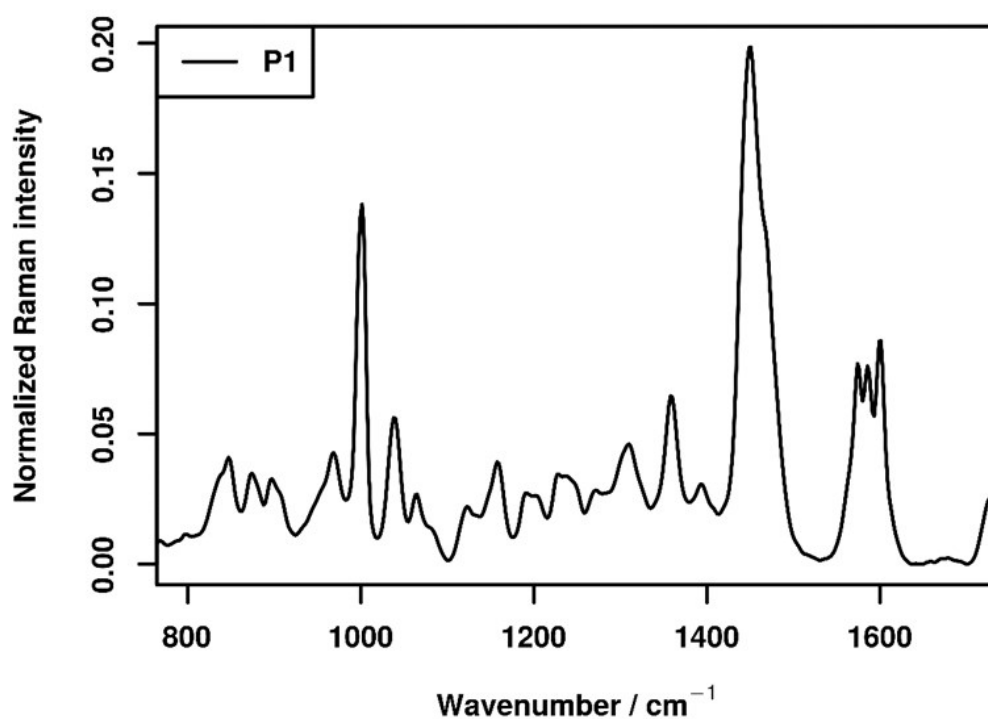


Figure S46. Raman spectrum of polymer **P1** in the wavenumber range between 800 and 1700 cm⁻¹.

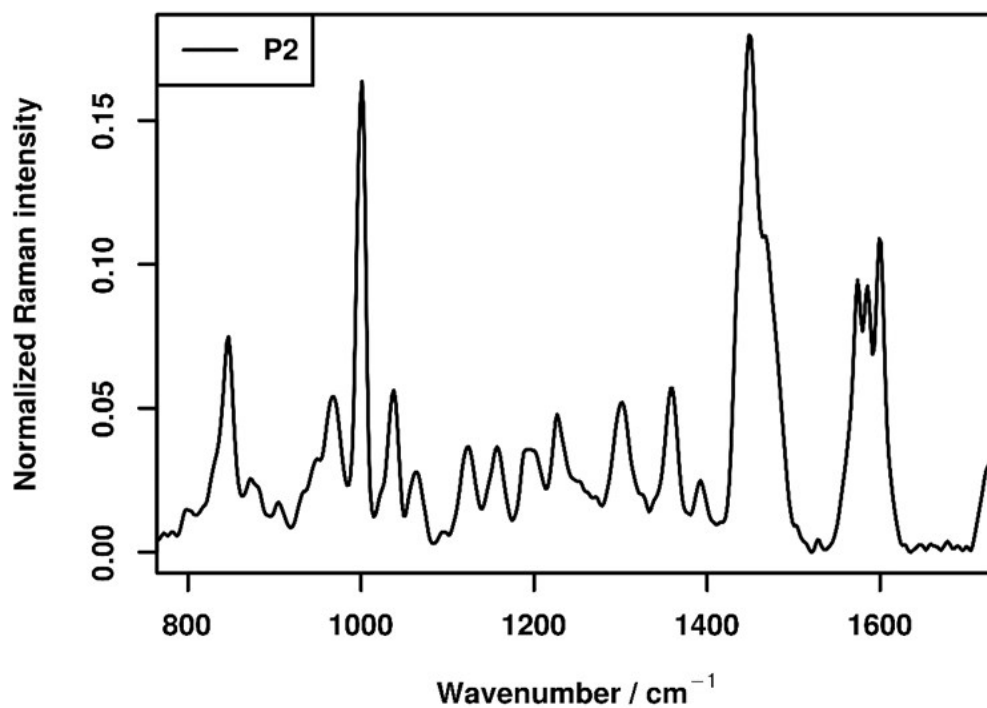


Figure S47. Raman spectrum of polymer **P2** in the wavenumber range between 800 and 1700 cm^{-1} .

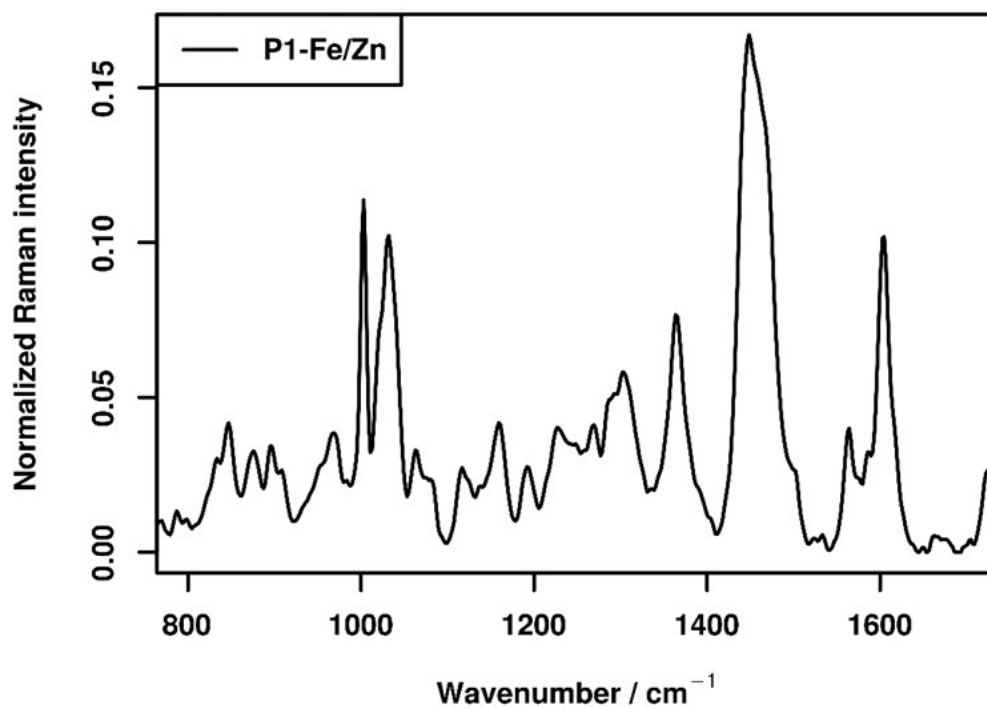


Figure S48. Raman spectrum of polymer **P1-Fe/Zn** in the wavenumber range between 800 and 1700 cm^{-1} .

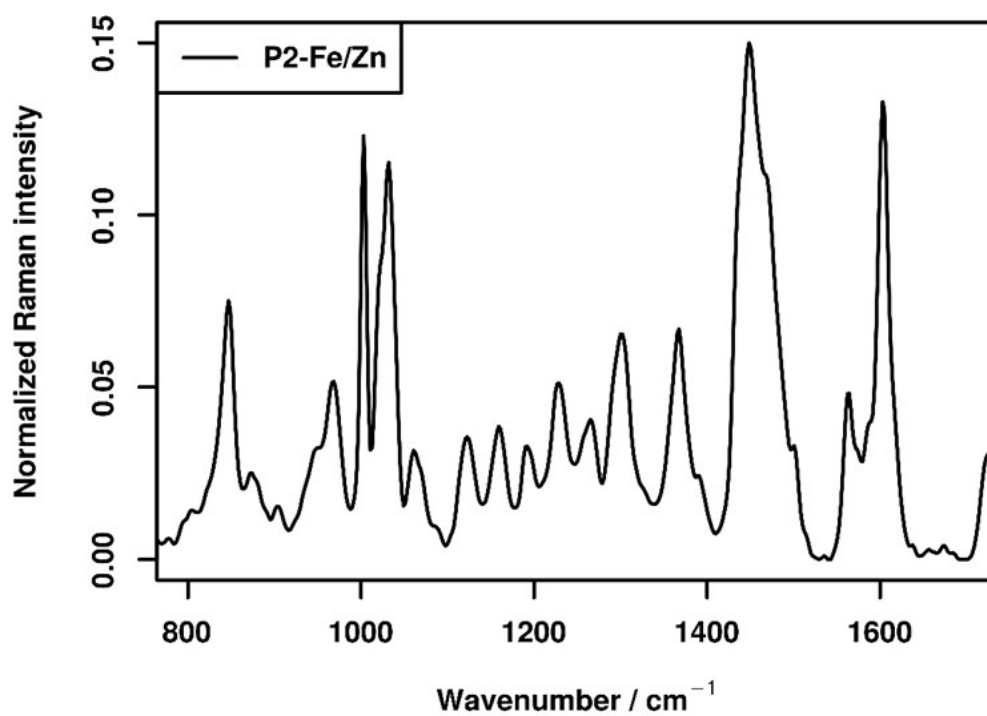


Figure S49. Raman spectrum of polymer **P2-Fe/Zn** in the wavenumber range between 800 and 1700 cm⁻¹.

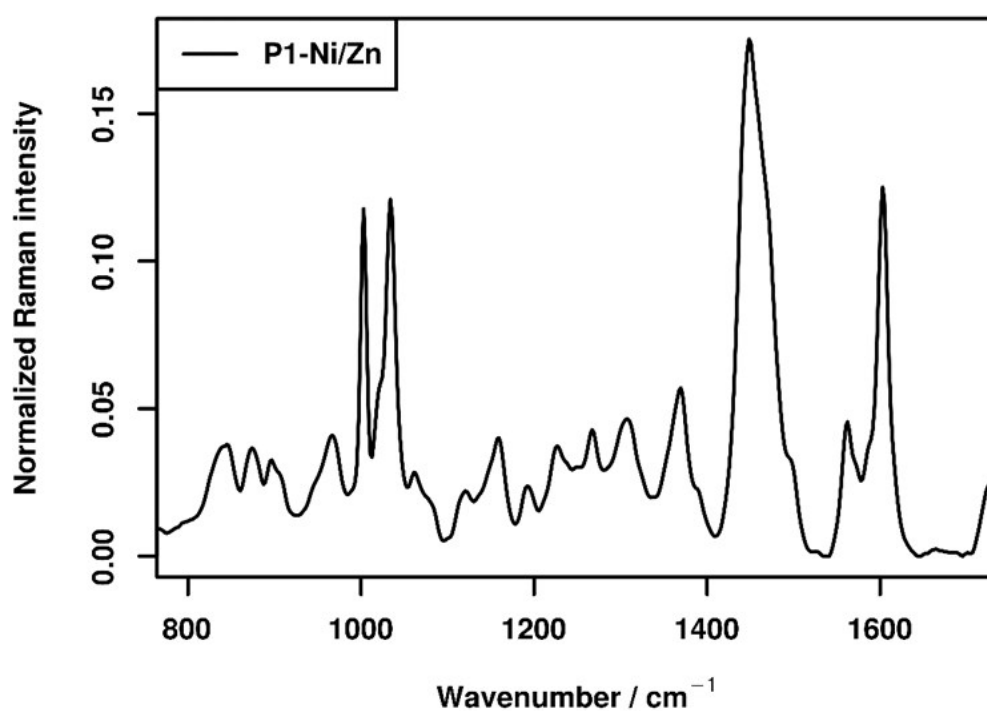


Figure S50. Raman spectrum of polymer **P1-Ni/Zn** in the wavenumber range between 800 and 1700 cm⁻¹.

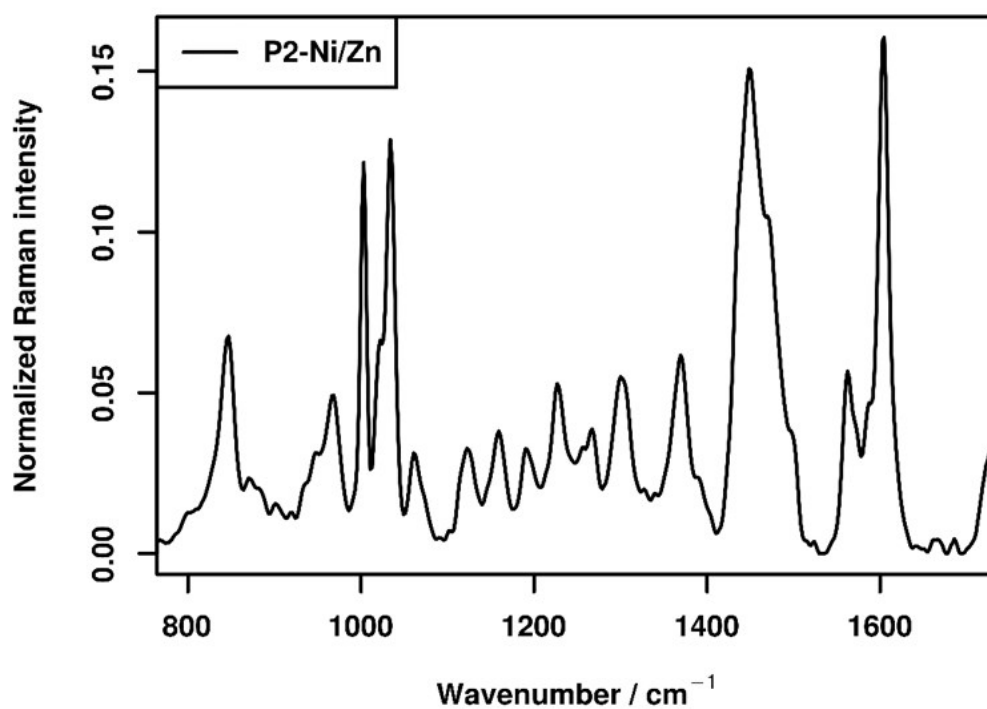


Figure S51. Raman spectrum of polymer **P2-Ni/Zn** in the wavenumber range between 800 and 1700 cm⁻¹.

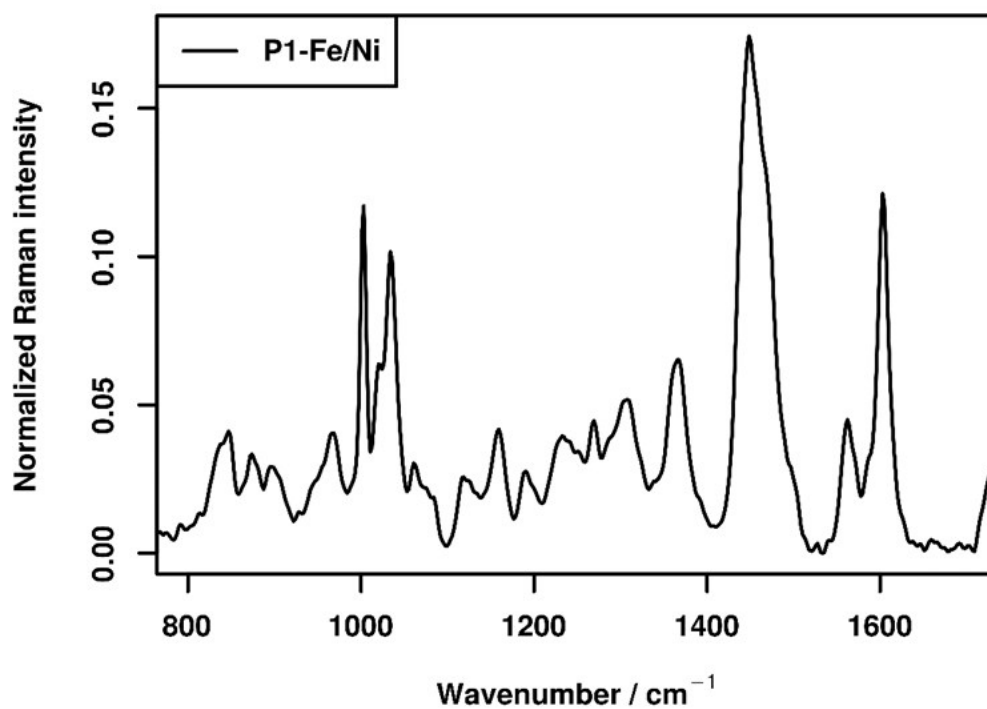


Figure S52. Raman spectrum of polymer **P1-Fe/Ni** in the wavenumber range between 800 and 1700 cm⁻¹.

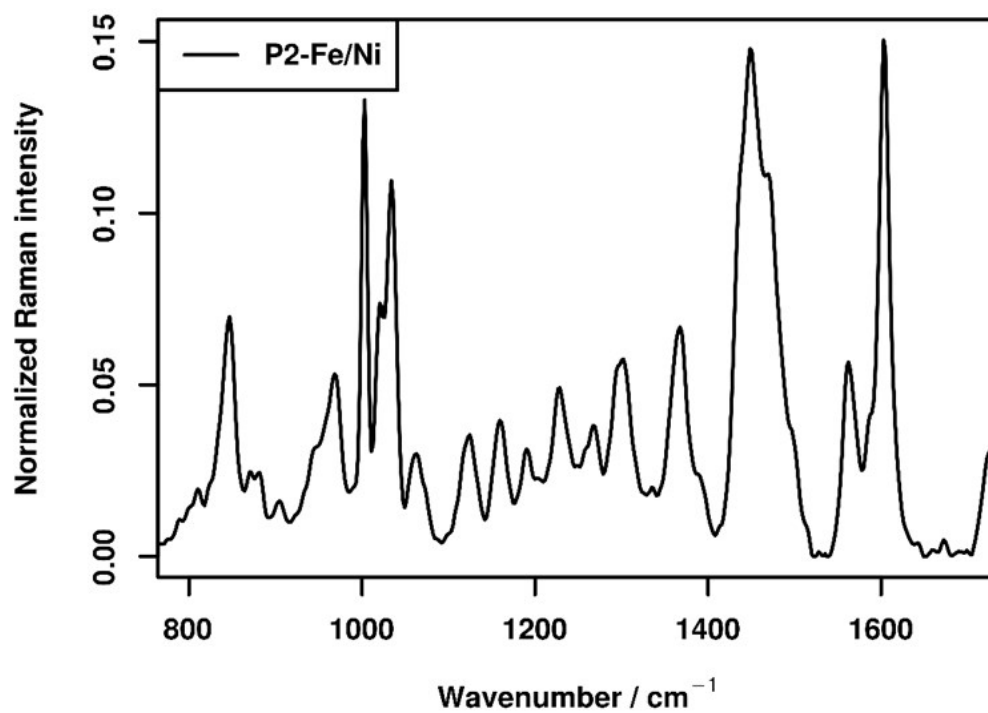


Figure S53. Raman spectrum of polymer **P2-Fe/Ni** in the wavenumber range between 800 and 1700 cm⁻¹.

Composition analysis by picture analysis

The polymer networks are challenging materials concerning their characterization because many solution based characterization methods fail for these crosslinked materials. In order to gain information about the formed complexes, the color of the materials can provide further information. Terpyridine complexes of different transition metal ions exhibit generally characteristic colors – for instance the iron(II)-*bis*-terpyridine complex is violet in solution. Consequently, also the herein presented metallopolymer networks feature significant differences regarding their color. Adapting the idea to investigate the color (red, green and blue content) presented in literature⁶⁻⁸ to gain information underlying processed or structural properties we qualitatively studied the utilized materials. For this purpose, photos of the polymers were taken under identical conditions. Subsequently, the red, green and blue-values were determined *via* paint.

To make these color differences comparable and to investigate, which metal-ion forms the complex with the terpyridine ligands the color composition of the metallopolymer networks as well as model metallopolymers was determined. Compared to the terpyridine complexes, the histidine complexes in general are only slightly colored and, thus, were neglected for the investigation of the color of the metallopolymer networks. Afterwards, photos of the shape-memory metallopolymer networks and the model metallopolymers were taken and the composition of the color was determined. The photos and the results of the red, green and blue content (RGB) is displayed in **Figure S53**. The metallopolymer networks **P1-Fe/Zn**, **P2-Fe/Zn**, **P1-Fe/Ni** and **P2-Fe/Ni**, in which a *bis*-terpyridine-iron(II) complex should form the stable phase have a very dark purple color, almost black. The model metallopolymer looks rather similar and color analysis revealed a comparable pattern. In contrast, the samples **P1-Ni/Zn** and **P2-Ni/Zn**, which should bear nickel(II)-*bis*-terpyridine complexes, appear rather yellowish brown. Compared to the model metallopolymer network **P_M-Ni** the red, green and blue content look quite similar. Regarding the model metallopolymers it was found that the ratio of red to green to blue in case of Ni-Tpy complexes is significantly larger compared to the Fe-Tpy complexes. This ratio between the colors was also found for **P1-Ni/Zn** and **P2-Ni/Zn**, indicating the formation of the desired Tpy-Ni complex. On the other hand, the determined ratio of red to green to blue for **P1-Fe/Zn**, **P2-Fe/Zn**, **P1-Fe/Ni** and **P2-Fe/Ni** is much smaller and more comparable with the ones found for **P_M-Fe**, indicating the formation of iron(II)-*bis*-terpyridine complexes. Within these results, it was possible to qualitatively proof the formation of the desired terpyridine complexes in the presented metallopolymer networks and to get insights into the molecular structure.

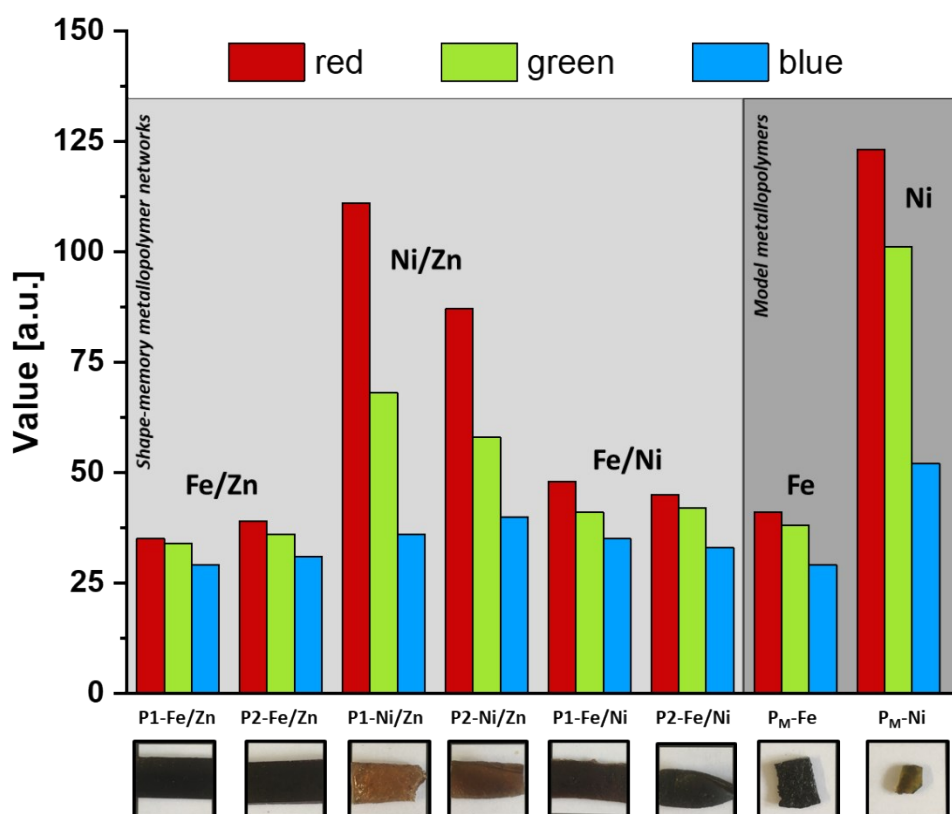


Figure S54. Determined color composition (RGB content) and corresponding photos of the metallopolymer networks **P1-Fe/Zn**, **P2-Fe/Zn**, **P1-Ni/Zn**, **P2-Ni/Zn**, **P1-Fe/Ni** and **P2-Fe/Ni** and model metallopolymer **P_M-Fe** and **P_M-Ni**.

References

1. S. Bode, L. Zedler, F. H. Schacher, B. Dietzek, M. Schmitt, J. Popp, M. D. Hager and U. S. Schubert, *Adv. Mater.*, 2013, **25**, 1634-1638.
2. M. Enke, F. Jehle, S. Bode, J. Vitz, M. J. Harrington, M. D. Hager and U. S. Schubert, *Macromol. Chem. Phys.*, 2017, **218**, 1600458.
3. J. Meurer, J. Hniopek, T. Bätz, S. Zechel, M. Enke, J. Vitz, M. Schmitt, J. Popp, M. D. Hager and U. S. Schubert, *Adv. Mater.*, 2021, **33**, 2006655.
4. R. Core Team R: A language and environment for statistical computing. R Foundation for Statistical Computing, Vienna, Austria. URL <https://www.R-project.org/>.
5. C. G. Ryan, E. Clayton, W. L. Griffin, S. H. Sie and D. R. Cousens, *Nucl. Instrum. Methods Phys. Res.*, 1988, **34**, 396-402.
6. W. Xu, S. Lu, Y. Chen, T. Zhao, Y. Jiang, Y. Wang and X. Chen, *Sens. Actuator B: Chem.*, 2015, **220**, 326-330.
7. L. H. Fischer, C. Karakus, R. J. Meier, N. Risch, O. S. Wolfbeis, E. Holder and M. Schäferling, *Chem. Eur. J.*, 2012, **18**, 15706-15713.
8. G. H. Darwish, H. H. Fakh and P. Karam, *The Journal of Physical Chemistry B*, 2017, **121**, 1033-1040.